

# Structure-Guided Design of A<sub>3</sub> Adenosine Receptor-Selective Nucleosides: Combination of 2-Arylethynyl and Bicyclo[3.1.0]hexane Substitutions

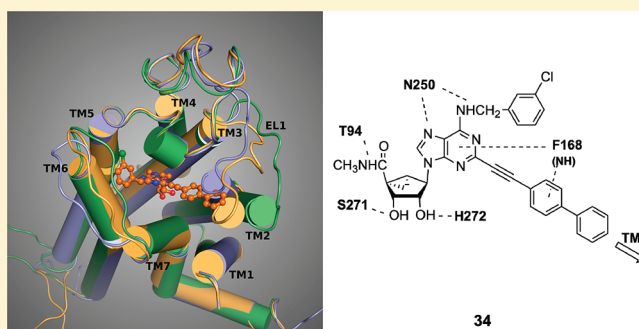
Dilip K. Tosh,<sup>†, §</sup> Francesca Deflorian,<sup>†, §</sup> Khai Phan,<sup>†</sup> Zhan-Guo Gao,<sup>†</sup> Tina C. Wan,<sup>‡</sup> Elizabeth Gizewski,<sup>‡</sup> John A. Auchampach,<sup>‡</sup> and Kenneth A. Jacobson<sup>\*,†</sup>

<sup>†</sup>Molecular Recognition Section, Laboratory of Bioorganic Chemistry, National Institute of Diabetes and Digestive and Kidney Diseases, National Institutes of Health, Bethesda, Maryland 20892, United States

<sup>‡</sup>Department of Pharmacology, Medical College of Wisconsin, 8701 Watertown Plank Road, Milwaukee, Wisconsin 53226, United States

## Supporting Information

**ABSTRACT:** (*N*)-Methanocarba adenosine 5'-methyluronamides containing known A<sub>3</sub> AR (adenosine receptor)-enhancing modifications, i.e., 2-(arylethynyl)adenine and *N*<sup>6</sup>-methyl or *N*<sup>6</sup>-(3-substituted-benzyl), were nanomolar full agonists of human (h) A<sub>3</sub>AR and highly selective (*K*<sub>i</sub> ~0.6 nM, *N*<sup>6</sup>-methyl 2-(halophenylethynyl) analogues **13** and **14**). Combined 2-arylethynyl-*N*<sup>6</sup>-3-chlorobenzyl substitutions preserved A<sub>3</sub>AR affinity/selectivity in the (*N*)-methanocarba series (e.g., 3,4-difluoro full agonist MRS5698 **31**, *K*<sub>i</sub> 3 nM, human and mouse A<sub>3</sub>) better than that for ribosides. Polyaromatic 2-ethynyl *N*<sup>6</sup>-3-chlorobenzyl analogues, such as potent linearly extended 2-*p*-biphenylethynyl MRS5679 **34** (*K*<sub>i</sub> hA<sub>3</sub> 3.1 nM; A<sub>1</sub>, A<sub>2A</sub>, inactive) and fluorescent 1-pyrene adduct MRS5704 **35** (*K*<sub>i</sub> hA<sub>3</sub> 68.3 nM), were conformationally rigid; receptor docking identified a large, mainly hydrophobic binding region. The vicinity of receptor-bound C2 groups was probed by homology modeling based on recent X-ray structure of an agonist-bound A<sub>2A</sub>AR, with a predicted helical rearrangement requiring an agonist-specific outward displacement of TM2 resembling opsin. Thus, the X-ray structure of related A<sub>2A</sub>AR is useful in guiding the design of new A<sub>3</sub>AR agonists.



## INTRODUCTION

The structure–activity relationship (SAR) of nucleoside agonists at the A<sub>3</sub> adenosine receptor (AR), a G protein-coupled receptor (GPCR) of the rhodopsin-like family A, has been extensively explored.<sup>1</sup> Several A<sub>3</sub>AR-selective agonists are currently in advanced clinical trials for the treatment of hepatocellular carcinoma, autoimmune inflammatory diseases,<sup>2–4</sup> such as rheumatoid arthritis, psoriasis, and dry eye disease, and other conditions.<sup>5–8</sup> Other potential applications of such agonists could be osteoarthritis, Crohn's disease, ischemia, and other inflammatory disorders. As applied to cancer models, there is evidence that multiple modes of benefit from A<sub>3</sub>AR agonists are obtained: myeloprotection and reduction of neuropathic pain, in addition to the antiproliferative effects on tumors in vivo. A<sub>3</sub>AR-selective antagonists are also of interest for therapeutic applications in asthma, glaucoma, septic shock, and other conditions.<sup>9–12</sup> Thus, this subtype of AR (others are A<sub>1</sub>AR, A<sub>2A</sub>AR, and A<sub>2B</sub>AR) has provided numerous opportunities for translation to therapeutics.

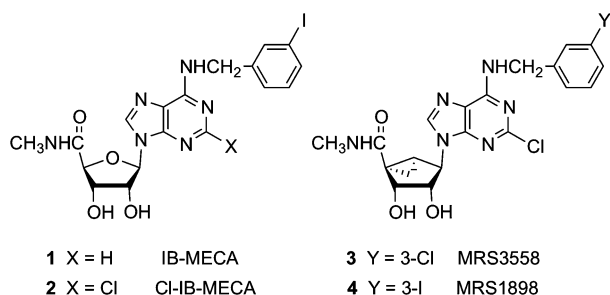
In order to achieve selectivity of adenosine derivatives for the A<sub>3</sub>AR, modifications are typically introduced on the *N*<sup>6</sup> position

(often *m*-substituted benzyl groups) and on the ribose moiety (often 5'-*N*-methyluronamide), such as occur on prototypical agonists **1** and **2** (Chart 1).<sup>13</sup> Replacement of the conformationally flexible ribose tetrahydrofuryl group with a rigid bicyclo[3.1.0]hexane (methanocarba) ring system in an isomeric form that enforces a North (*N*) envelope conformation increases both the binding affinity and selectivity of adenosine derivatives as A<sub>3</sub>AR agonists.<sup>14–16</sup> For example, analogues that combined *N*<sup>6</sup>-(3-halobenzyl) and (*N*)-methanocarba modifications, such as **3** and **4**, display anti-inflammatory activity, protection in a model of lung injury, and protection against chemotherapy-induced neuropathic pain.<sup>17–19</sup> Cristalli and co-workers have explored the SAR leading to enhancement of A<sub>2A</sub>AR and A<sub>3</sub>AR affinity by alkyn-2-yl groups, such as hexyn-2-yl, at the adenine C2 position of adenine 9-ribosides.<sup>20</sup> The enhancement of human (h) A<sub>3</sub>AR affinity by such groups was also observed in the (*N*)-methanocarba series.<sup>21</sup> Because ligand affinity at the A<sub>3</sub>AR is often dependent on species, it was particularly important to

Received: March 21, 2012

Published: May 4, 2012

**Chart 1. Derivatives of Adenosine as A<sub>3</sub>AR-Selective Agonists in the Ribose (1,2) and (N)-Methanocarpa (3,4) Series**



establish the effect in species other than humans. The combination of N<sup>6</sup>-(3-halobenzyl), 2-alkyn-2-yl, and 5'-N-methyluronamide modifications was found to be particularly well suited for application to agonists displaying A<sub>3</sub>AR selectivity across species.

There is a precedent for the lack of compatibility in AR recognition of multiple modifications of nucleoside derivatives at the N<sup>6</sup> (i.e., 3-halobenzyl) and C2 positions (i.e., aryl or large hydrophobic groups), each of which may promote affinity at A<sub>3</sub>AR and other subtypes.<sup>13,22</sup> There is also indication that N<sup>6</sup>-3-(substituted benzyl) and 2-arylethynyl (introduced by Cristalli and colleagues<sup>23</sup>) modifications are not additive in their effect on A<sub>3</sub>AR selectivity of 9-ribosides.<sup>24</sup> The present

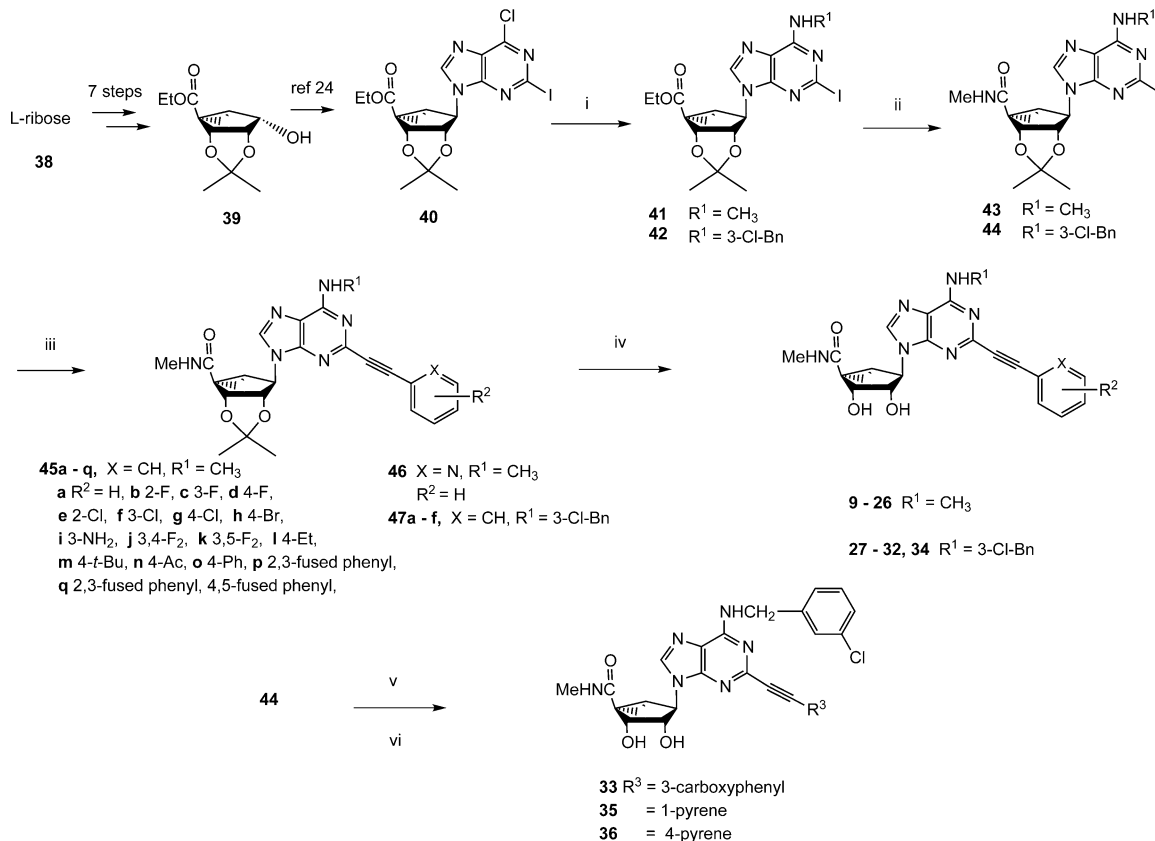
study establishes that these two substitutions are fully additive and conducive to high selectivity when applied to (N)-methanocarpa adenosine derivatives. We have also used molecular modeling based on a recent X-ray structure of an A<sub>2A</sub>AR complex with a 5',2',N<sup>6</sup> trisubstituted agonist<sup>25,26</sup> and with insights from other GPCRs<sup>26</sup> to probe the vicinity of the 2-arylethynyl groups when docked to the A<sub>3</sub>AR. Thus, the crystallographic structure of one AR subtype is used to guide the design of new analogues at another AR subtype following necessary customization for this ligand set.

## RESULTS

**Chemical Synthesis.** We have explored 2-arylethynyl substitution of the adenine ring of previously reported (N)-methanocarpa 5'-N-methyluronamide nucleoside derivatives that act as selective A<sub>3</sub>AR agonists.<sup>14,15,21</sup> Two series, depending on the N<sup>6</sup> substitution (N<sup>6</sup>-methyl, 8–26, and N<sup>6</sup>-3-chlorobenzyl, 27–36), that are closely patterned on known potent agonists are included (Scheme 1). N<sup>6</sup>-Methyladenosines are typically significantly more potent at the hA<sub>3</sub>AR than at rat (r) A<sub>3</sub>AR, while N<sup>6</sup>-(3-halobenzyl)adenosines tend to display greater species-independent selectivity.

The synthetic route used to prepare (N)-methanocarpa 5'-N-methyluronamido derivatives containing a 2-arylethynyl group involved a key Sonogashira reaction<sup>27</sup> at a 2-iodoadenine moiety of intermediate 43 or 44 (Scheme 1). L-Ribose 38 was converted as previously reported into the 2',3'-protected

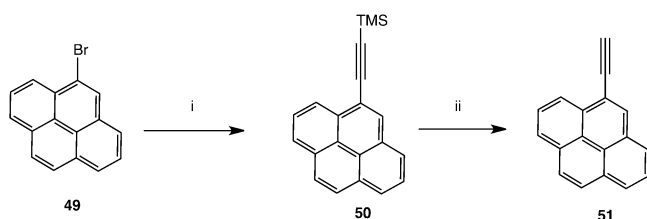
**Scheme 1. Synthesis of (N)-Methanocarpa Nucleoside Analogues<sup>a</sup>**



<sup>a</sup>R<sub>1</sub> = Me or 3-Cl-benzyl. Reagents: (i) MeNH<sub>2</sub> or 3-Cl-benzylamine, Et<sub>3</sub>N, MeOH, rt; (ii) 40% MeNH<sub>2</sub>, MeOH, rt; (iii) HC≡CAr, Pd(PPh<sub>3</sub>)<sub>2</sub>Cl<sub>2</sub>, CuI, Et<sub>3</sub>N, DMF, rt; (iv) 10% TFA, MeOH, 70 °C; (v) 1-ethynylpyrene or 4-ethynylpyrene 51, Pd(PPh<sub>3</sub>)<sub>2</sub>Cl<sub>2</sub>, CuI, Et<sub>3</sub>N, DMF, rt; (vi) 1 N, HCl, dioxane, 60 °C.

intermediate **39** containing a 5-ethyl ester, which was then subjected to a Mitsunobu condensation with 2-iodo-6-chloropurine to give **40**.<sup>21,28</sup> A *N*<sup>6</sup>-methyl or *N*<sup>6</sup>-(3-chlorobenzyl) group was added by nucleophilic substitution of 6-chloro at room temperature to provide intermediates **41** and **42**, respectively, followed by aminolysis of the ester at room temperature leading to 5'-*N*-methyluronamides **43** and **44**. A Sonogashira reaction was then carried out with a variety of commercially available arylacetylenes to give protected nucleosides **45–46** (*N*<sup>6</sup>-methyl) and **47a–f** (*N*<sup>6</sup>-3-chlorobenzyl). Finally, acid hydrolysis of the isopropylidene protecting group provided *N*<sup>6</sup>-methyl **9–26** and *N*<sup>6</sup>-3-chlorobenzyl **27–36** nucleosides. The associated synthesis of a polyaromatic ethynyl intermediate **51** is shown in Scheme 2.

**Scheme 2. Synthesis of an Intermediate Arylalkynyl Derivative<sup>a</sup>**



<sup>a</sup>(i)  $\text{HC}\equiv\text{C-TMS}$ ,  $\text{Pd}(\text{PPh}_3)_2\text{Cl}_2$ ,  $\text{CuI}$ ,  $\text{Et}_3\text{N}$ ,  $\text{DMF}$ ,  $\text{rt}$ ; (ii)  $\text{TBAF}$ ,  $\text{THF}$ .

**Pharmacological Activity.** Radioligand binding assays at three hAR subtypes were carried out using standard <sup>3</sup>H (**52**, **53**) and <sup>125</sup>I-labeled (**54**) nucleosides (Table 1).<sup>29–31</sup> The membrane preparations were obtained from Chinese hamster ovary (CHO) cells (*A*<sub>1</sub> and *A*<sub>3</sub>) or human embryonic kidney (HEK293) cells (*A*<sub>2A</sub>) stably expressing a hAR subtype.<sup>28,29,32,33</sup> *A*<sub>3</sub>AR binding curves generally showed a Hill coefficient of ~1. The nucleoside analogues were not all screened for activity at the *hA*<sub>2B</sub>AR because other (*N*)-methanocarba nucleosides were previously noted to be very weak or inactive at that subtype.<sup>15</sup> For example, in cyclic AMP assays, agonist **3** displayed 30,000-fold selectivity for the *hA*<sub>3</sub>AR in comparison to the *hA*<sub>2B</sub>AR.<sup>17</sup> Some previously reported 2-chloro and 2-alkynyl (*N*)-methanocarba agonists (**3–8**) were used for comparison in the biological assays.<sup>20</sup> For exploring species differences in AR ligand recognition, binding assays were also performed on selected nucleoside derivatives at three mouse (m) ARs (Table 2) expressed in HEK293 cells.<sup>21,33b</sup>

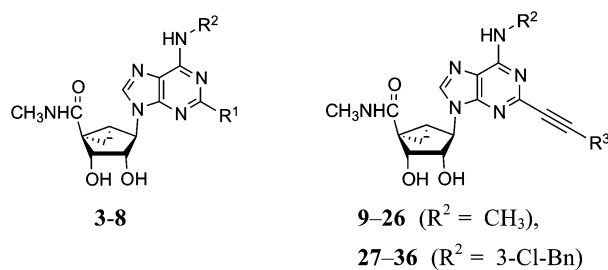
The simplest *N*<sup>6</sup>-methyl 2-phenylethynyl analogue **9** displayed a subnanomolar *K*<sub>i</sub> value at the *hA*<sub>3</sub>AR and was nearly inactive at the *hA*<sub>1</sub>AR and *hA*<sub>2A</sub>AR, with <20% inhibition of binding at 10 μM. Therefore, the degree of *A*<sub>3</sub>AR selectivity of **9** was estimated to be >10,000-fold. The effects of phenyl modification of the C2-arylethynyl group at the C2 position were explored initially in the *N*<sup>6</sup>-methyl 5'-*N*-methyluronamide series. These derivatives displayed great freedom of substitution of the arylethynyl moiety, i.e., aza substitution of a CH of phenyl (**10**), monohalo (**11–17**) and dihalo (**19**, **20**) or other (**18**, **21–23**) substituent groups on the phenyl ring, and the presence of additional aryl rings (**24–26**). The 3,4-difluorophenyl analogue **19** was particularly *A*<sub>3</sub>AR-selective with insignificant inhibition at *A*<sub>1</sub> and *A*<sub>2A</sub>ARs. Planar polyaromatic groups, such as  $\alpha$ -naphthyl **25** and the larger phenanthrene **26**, in the *N*<sup>6</sup>-methyl series did not interfere with the binding to the

*hA*<sub>3</sub>AR. The presence of a branched *p-t*-Bu group in **22** reduced *A*<sub>3</sub>AR binding affinity by 12-fold compared to the H analogue **9**. The most potent *A*<sub>3</sub>AR ligands in the *N*<sup>6</sup>-methyl series were halo-substituted compounds **13** and **14** with *K*<sub>i</sub> values of 0.5–0.6 nM. A *p*-acetyl substitution in **23** was lower in *hA*<sub>3</sub>AR affinity and higher in *hA*<sub>2A</sub>AR affinity than most other ring substitutions, unlike in the riboside series of Cristalli and co-workers,<sup>23a</sup> in which a 2(-*p*-acetylphenylethynyl) group favored *A*<sub>3</sub>AR affinity and selectivity.

The variability of binding affinity upon substitution of the arylethynyl moiety was greater at the *hA*<sub>2A</sub>AR than at the *hA*<sub>1</sub>AR. For example, the *hA*<sub>2A</sub>AR affinity increased substantially to a *K*<sub>i</sub> value of 1.3 μM upon replacement of 3-F **12** with 3-Cl in **15**. In contrast, the same change slightly decreased *hA*<sub>3</sub>AR affinity. At the *hA*<sub>1</sub>AR, only 10 to 30% of binding inhibition was typically seen at 10 μM for a variety of substitutions.

The SAR was extended by the analysis of 11 analogues prepared in the *N*<sup>6</sup>-(3-chlorobenzyl) series (**27–36**). The effect in **27** of adding a phenyl group to the ethynyl substituent of the simpler acetylene derivative **6** was complete retention of the affinity at *hA*<sub>3</sub>AR and a reduction of the *hA*<sub>1</sub>AR affinity from *K*<sub>i</sub> = 174 nM to >10 μM, thus providing high selectivity. Furthermore, with only marginal binding of **27** at the *hA*<sub>2A</sub>AR, the *hA*<sub>3</sub>AR selectivity was roughly 10,000-fold in comparison to both *hA*<sub>1</sub>AR and *hA*<sub>2A</sub>AR. For comparison, by adding a *n*-propyl chain in **7** rather than a phenyl ring, the *hA*<sub>1</sub>AR affinity was reduced only 6-fold in comparison to **6**, and the *hA*<sub>2A</sub>AR affinity appeared to be increased. Thus, a flat aryl ring rather than a flexible alkyl chain provides the appropriate geometry for *hA*<sub>3</sub>AR selectivity. A potent *A*<sub>3</sub>AR ligand **34** in the *N*<sup>6</sup>-(3-chlorobenzyl) series containing a rigid, linearly extended 2-*p*-biphenylethynyl group served as a model ligand for receptor docking due to its steric and conformational constraints. It displayed a *K*<sub>i</sub> value at the *hA*<sub>3</sub>AR of 3.06 nM and exceptionally high selectivity in comparison to the *hA*<sub>1</sub> and *hA*<sub>2A</sub>ARs (no inhibition observed). The *hA*<sub>3</sub>AR affinities of biphenyl derivative **34** and the corresponding *N*<sup>6</sup>-methyl analogue **24** were equal. The affinity of the pyrene adducts **35** and **36** depended on the position of substitution. Thus, the combination of 2-arylethynyl, 5'-*N*-methyluronamide, and *N*<sup>6</sup>-3-chlorobenzyl substitution preserved the *hA*<sub>3</sub>AR selectivity of (*N*)-methanocarba nucleosides, even for large 2-arylethynyl moieties.

Species differences in the binding affinity of the nucleoside derivatives were explored. Nanomolar *A*<sub>3</sub>AR affinity was maintained in a murine species only for the *N*<sup>6</sup>-(substituted benzyl) series (Figure 1). The *N*<sup>6</sup>-methyl-2-arylethynyl derivatives **13** and **14** were determined to be ~70-fold weaker at the *mA*<sub>3</sub>AR than at the *hA*<sub>3</sub>AR, consistent with the previously reported reduced affinity at *mA*<sub>3</sub>AR of *N*<sup>6</sup>-methyl-2-Cl derivative **8**.<sup>21</sup> The *mA*<sub>3</sub>AR/*mA*<sub>1</sub>AR selectivity in the *N*<sup>6</sup>-methyl series was enhanced with the elongation and rigidification of the C2 substituent. However, with *N*<sup>6</sup>-3-chlorobenzyl substitution, elongation at C2 did not significantly reduce affinity at the *mA*<sub>3</sub>AR compared to *hA*<sub>3</sub>AR (except for a 3-fold reduction for the elongated biaryl derivative **34**). In the *N*<sup>6</sup>-3-chlorobenzyl series, particularly high selectivity compared to *mA*<sub>1</sub>AR and *mA*<sub>2A</sub>AR was generally present. There was greater variability in the degree of binding inhibition at *mA*<sub>1</sub>AR than at *mA*<sub>2A</sub>AR. Elongation of a 2-ethynyl group in **6** with a straight alkyl chain in **7** reduced *mA*<sub>3</sub>AR affinity by 7-fold, but elongation with a phenyl ring in **27** only slightly reduced

Table 1. Binding Affinity of a Series of (*N*)-Methanocarba Adenosine Derivatives at Three Subtypes of hARs and the Functional Efficacy at the hA<sub>3</sub>AR

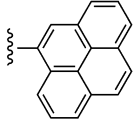
Compd	Structure		Affinity ( $K_i$ , nM) or % inhibition <sup>a</sup>			%Efficacy <sup>b</sup>
	R <sup>1</sup> or R <sup>3</sup>	R <sup>2</sup>	hA <sub>1</sub>	hA <sub>2A</sub>	hA <sub>3</sub>	hA <sub>3</sub>
3 <sup>c</sup>	Cl	3-Cl-Bn	260±60	2300±100	0.29±0.04	103±7
4 <sup>c,d</sup>	Cl	3-I-Bn	136±22	784±97	1.5±0.2	100
5 <sup>c</sup>	H	3-I-Bn	700±270	6200±100	2.4±0.5	100
6 <sup>d</sup>	C≡CH	3-Cl-Bn	174±23	(48%)	1.30±0.38	ND
7 <sup>d</sup>	C=C(CH <sub>2</sub> ) <sub>2</sub> CH <sub>3</sub>	3-Cl-Bn	1040±83	(80%)	0.82±0.20	ND
8 <sup>c,d</sup>	Cl	CH <sub>3</sub>	2100±1700	(6%)	2.2±0.6	ND
9		CH <sub>3</sub>	(13%±6%)	(14%±7%)	0.85±0.22	89.3±7.7
10		CH <sub>3</sub>	(11%±4%)	(13%±4%)	1.01±0.36	86.8±9.2
11		CH <sub>3</sub>	(21%±4%)	(17%±2%)	0.97±0.38	97.7±9.1
12		CH <sub>3</sub>	(12%±2%)	(10%±5%)	0.97±0.24	95.8±6.7
13		CH <sub>3</sub>	(21%±11%)	(19%±3%)	0.53±0.09	80.3±5.8
14		CH <sub>3</sub>	(27%±7%)	(30%±5%)	0.58±0.04	84.2±6.2
15 <sup>c</sup>		CH <sub>3</sub>	(10%±2%)	1270±300	1.60±0.60	90.9±1.9
16		CH <sub>3</sub>	(14%±1%)	(30%±1%)	1.22±0.31	97.4±9.1
17		CH <sub>3</sub>	(13%±7%)	(26%±1%)	0.91±0.06	97.5±12.3
18		CH <sub>3</sub>	(10%±5%)	(19%±14%)	1.07±0.14	109±4.1
19		CH <sub>3</sub>	(6%±3%)	(6%±6%)	1.65±0.08	108±1.9

Table 1. continued

Compd	Structure		Affinity ( $K_{i5}$ , nM) or % inhibition <sup>a</sup>			%Efficacy <sup>b</sup>
	R <sup>1</sup> or R <sup>3</sup>	R <sup>2</sup>	hA <sub>1</sub>	hA <sub>2A</sub>	hA <sub>3</sub>	hA <sub>3</sub>
20		CH <sub>3</sub>	(8%±3%)	(47%±4%)	1.66±0.36	99.6±3.3
21		CH <sub>3</sub>	(13%±3%)	(38%±5%)	3.78±1.16	110±4.9
22		CH <sub>3</sub>	(23%±5%)	(7%±5%)	10.1±1.9	78.4±6.5
23 <sup>c</sup>		CH <sub>3</sub>	(15%±7%)	5300±600	2.57±0.78	87.4±9.9
24		CH <sub>3</sub>	(21%±6%)	(29%±8%)	3.10±1.26	110±2.9
25		CH <sub>3</sub>	(25%±1%)	(34%±8%)	1.67±0.18	94.6±4.4
26		CH <sub>3</sub>	(15%±5%)	(52%±1%)	3.48±1.36	108±3.5
27		3-Cl-Bn	(20%±3%)	(27%±3%)	1.34±0.30	101±5.9
28 <sup>c</sup>		3-Cl-Bn	(20%±6%)	(42%±2%)	2.16±0.34	102±1.4
29		3-Cl-Bn	(19%±2%)	(52%±12%)	1.92±0.57	103±1.5
30 <sup>c</sup>		3-Cl-Bn	(4%±4%)	1740±590	4.45±1.39	91.5±11.4
31 <sup>c</sup>		3-Cl-Bn	(6%±4%)	(41%±10%)	3.49±1.84	95.7±6.4
32		3-Cl-Bn	1520±300	(44%±4%)	2.27±0.70	76.6±13.1
33		3-Cl-Bn	(6%±5%)	(38%±5%)	6.75±2.78	86.7±5.4
34		3-Cl-Bn	(2%±2%)	(0%±0%)	3.06±1.35	89.0±4.5
35 <sup>c</sup>		3-Cl-Bn	(8%±2%)	3110±530	68.3±12.5	77.8±11.6



Table 1. continued

Compd	Structure		Affinity ( $K_i$ , nM) or % inhibition <sup>a</sup>			%Efficacy <sup>b</sup>
	R <sup>1</sup> or R <sup>3</sup>	R <sup>2</sup>	hA <sub>1</sub>	hA <sub>2A</sub>	hA <sub>3</sub>	hA <sub>3</sub>
36		3-Cl-Bn	(11% ± 5%)	(4% ± 3%)	660 ± 170	97.1 ± 3.3

<sup>a</sup>All experiments were done on CHO or HEK293 (A<sub>2A</sub> only) cells stably expressing one of three subtypes of the four hARs. The binding affinity for A<sub>1</sub>, A<sub>2A</sub>, and A<sub>3</sub>ARs was expressed as  $K_i$  values ( $n = 3-5$ ) and was determined by using agonist radioligands (<sup>3</sup>H]<sup>N</sup><sup>6</sup>-R-phenylisopropyladenosine 52 (R-PIA), [<sup>3</sup>H]2-[*p*-(2-carboxyethyl)phenyl-ethylamino]-5'-N-ethylcarboxamidoadenosine 53 (CGS21680), or [<sup>125</sup>I]<sup>N</sup><sup>6</sup>-(4-amino-3-iodobenzyl)-adenosine-5'-N-methyluronamide 54 (1-AB-MECA), respectively), unless noted.<sup>29-31</sup> The percent value in parentheses refers to inhibition of radioligand binding at 10 μM ( $n = 3$ ). ND, not determined. <sup>b</sup>Unless noted, the efficacy at the hA<sub>3</sub>AR was determined by inhibition of forskolin-stimulated cAMP production in AR-transfected CHO cells.<sup>32-34</sup> At a concentration of 10 μM, in comparison to the maximal effect of 5'-N-ethylcarboxamidoadenosine 48 (=100%) at 10 μM. Data are expressed as the mean ± standard error ( $n = 3$ ). <sup>c</sup>Values from Lee et al. and Tchilibon et al.<sup>15,16</sup> <sup>d</sup>Values from Melman et al.<sup>21</sup> <sup>e</sup>The relative efficacy (10 μM) at the hA<sub>2B</sub>AR (cyclic AMP accumulation) was 20–30% of full agonist 48.

Table 2. Binding Affinity of a Series of (*N*)-Methanocarba Adenosine Derivatives at Three Subtypes of mARs

compd	affinity ( $K_i$ , nM) or % inhibition <sup>a</sup>		
	mA <sub>1</sub>	mA <sub>2A</sub>	mA <sub>3</sub>
3 <sup>b</sup>	15.3 ± 5.8	10,400 ± 1,700	1.49 ± 0.46
4 <sup>b</sup>	7.32 ± 1.5	5,350 ± 860	0.80 ± 0.14
6 <sup>b</sup>	45.6 ± 7.9	(41%) <sup>j</sup>	0.85 ± 0.08
7 <sup>b</sup>	1390 ± 430	(42%) <sup>j</sup>	6.06 ± 1.21
8 <sup>b</sup>	55.3 ± 6.0	20,400 ± 3,200	49.0 ± 3.9
13	(29 ± 2%)	(0%)	37.7 ± 1.1
14	(55 ± 5%)	(2 ± 1%)	37.2 ± 2.0
27	(50 ± 5%)	(2 ± 1%)	1.23 ± 0.14
28	(65 ± 3%)	(7 ± 2%)	2.38 ± 0.04
29	(51 ± 12%)	(19 ± 3%)	2.64 ± 0.22
30	(35 ± 3%)	(55%)	2.39 ± 0.38
31	(14 ± 3%)	(27 ± 2%)	3.08 ± 0.23
32	261 ± 19	(5 ± 2%)	0.82 ± 0.06
33	(18 ± 3%)	(22%)	3.66 ± 0.25
34	(41 ± 6%)	(6 ± 1%)	10.8 ± 0.93
35	(8 ± 2%)	(64%)	47.6 ± 4.6

<sup>a</sup>Competition radioligand binding assays using [<sup>125</sup>I]54 (A<sub>1</sub> and A<sub>3</sub>ARs) and [<sup>3</sup>H]53 (A<sub>2A</sub>AR) were conducted with membranes prepared from HEK293 cells expressing recombinant mA<sub>1</sub>, mA<sub>2A</sub>, or mA<sub>3</sub>ARs. The data ( $n = 3-4$ ) are expressed as  $K_i$  values. The percent value in parentheses refers to the inhibition of radioligand binding at 10 μM. <sup>b</sup>Values from Melman et al.<sup>21</sup>

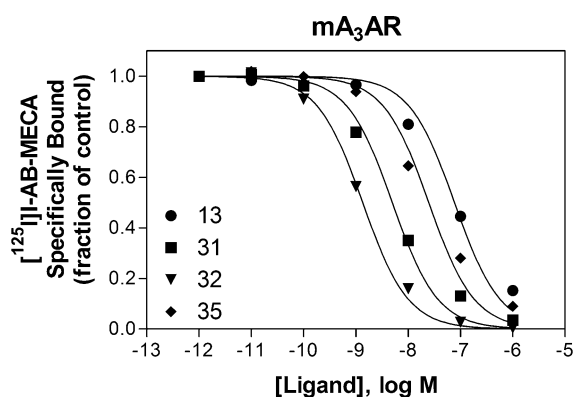


Figure 1. Inhibition of binding of the radioligand [<sup>125</sup>I]54 (0.3 nM) at the mA<sub>3</sub>AR by compounds 13, 31, 32, and 34.  $K_i$  values are found in Table 2.

mA<sub>3</sub>AR affinity. The most potent derivative at the mA<sub>3</sub>AR was the *p*-aminophenyl analogue 32 with a  $K_i$  value of 0.82 nM. Curiously, although this derivative remained selective, its A<sub>1</sub>AR affinity was enhanced over other members of the series at both in mouse ( $K_i$  261 nM) and human ( $K_i$  1520 nM).

Functional data were determined in an assay consisting of hA<sub>3</sub>AR-induced inhibition of the production of adenosine 3',5'-cyclic phosphate (cAMP) in membranes of CHO cells expressing the hA<sub>3</sub>AR (Table 1).<sup>34</sup> Inhibition by 10 μM NECA (48, 5'-N-ethylcarboxamidoadenosine) was set at 100% relative efficacy. The novel (*N*)-methanocarba 5'-N-methyluronamide derivatives at 10 μM were predominantly full agonists at the A<sub>3</sub>AR, with a few analogues showing relative efficacy of 80% or less (*p*-fluoro 13, *t*-butyl-phenyl 22, and 1-pyrene 35 derivatives). A full concentration–response curve in hA<sub>3</sub>AR-mediated inhibition of adenylate cyclase for 3,4-difluoro analogue 31 provided an EC<sub>50</sub> value of 1.2 ± 0.7 nM (Figure 2), i.e., slightly more potent than its binding affinity. Although weak in binding, the pyren-4-yl derivative 36 was fully efficacious.

**Molecular Modeling.** A homology model of the hA<sub>3</sub>AR based on an agonist-bound hA<sub>2A</sub>AR X-ray structure (PDB code 3QAK)<sup>25</sup> was used to study the putative interactions between the C2-substituted agonist 34 and the A<sub>3</sub>AR. The binding mode of 34 obtained after Induced Fit Docking (IFD)<sup>35</sup> revealed the following binding interactions of the ligand (Figure 3). The key

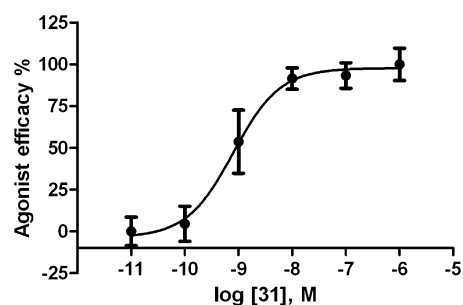
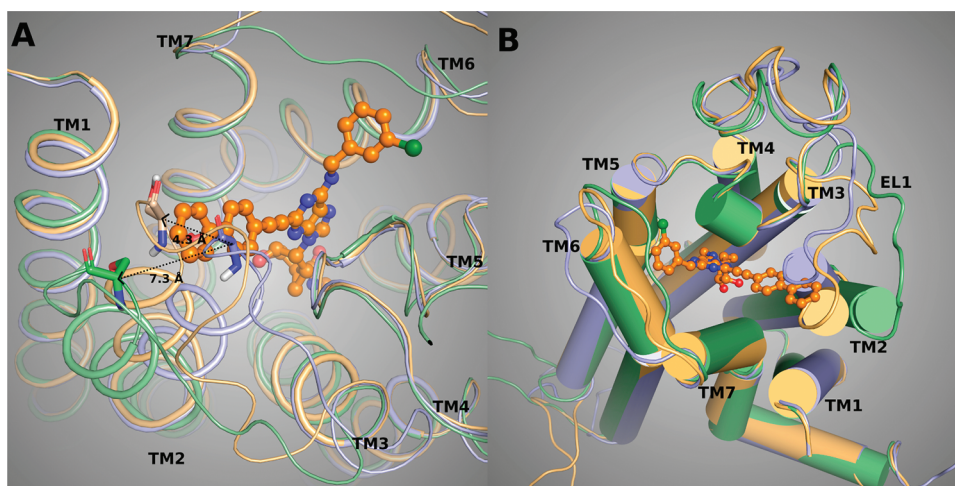


Figure 2. Functional agonism tested in an assay of adenylate cyclase in membranes of CHO cells expressing hA<sub>3</sub>AR. Activity of the 2-(3,4-difluorophenylethynyl)-N<sup>6</sup>-3-chlorobenzyl-5'-N-methyluronamide-(*N*)-methanocarba analogue 31 (EC<sub>50</sub> value 1.2 ± 0.7 nM). The full agonist 5'-N-ethyluronamidoadenosine 48 was included for comparison (representing 100% efficacy). The experiment was repeated three times, and the average is shown.



**Figure 3.** Binding mode (two different views with (A) wire helices and (B) tube helices) of linearly extended  $N^6$ -3-chlorobenzyl analogue **34** obtained after IFD to the  $A_3$ AR homology model. The template was built based on the crystal structure of an agonist-bound  $A_{2A}$ AR (purple helices)<sup>25</sup> and adjusted for movement of TM2 based on other templates ( $\beta_2$ -adrenergic receptor, brown helices; opsin, green helices).<sup>40,41</sup> The most successful template for TM2 was the structure of opsin.

residues embedding the adenosine moiety of the agonists in the receptor binding site are mostly conserved among AR subtypes. The 3'- and 2'-hydroxyl groups were located in proximity to Ser271 (7.42) and His272 (7.43), respectively, and could form H-bonds with these residues. The NH group of the  $S$ - $N$ -methylcarboxamido moiety was involved in H-bonding with the side chain hydroxyl group of Thr94 (3.36). Both the 6-amino group and the N7 atom of the adenine ring H-bond with Asn250 (6.55). A  $\pi$ - $\pi$  interaction was observed between the adenine ring of **34** and Phe168 (EL2), while the side chains of Leu246 (6.51) and Ile268 (7.39) offered CH- $\pi$  interactions to the adenine moiety of **34**. The ligand-receptor interactions observed in the present model were in good agreement with the data of site-directed mutagenesis and with our previously published models of ARs, including the studies of AR agonists docked to the  $A_{2A}$ AR crystal structure.<sup>36-38</sup> In the model obtained, the 3-chlorobenzyl ring of docked **34** was located in the hydrophobic pocket formed by Val169 (EL2), Met174 (5.35), Met172 (5.33), Ile253 (6.58), and Leu264 (7.35). More precisely, the  $N^6$ -3-chlorobenzyl substituent of **34** was locked in the hydrophobic pocket of the  $A_3$ AR among TMs5, TM6, TM7, and EL2 by CH- $\pi$  interactions with the side chains of Val169 (EL2) and Ile253 (6.58). Ile253 (6.58) is not conserved among the ARs: in  $A_1$ ,  $A_{2A}$ , and  $A_{2B}$ , the residue at position 6.58 is a smaller threonine. Moreover, favorable interactions between the backbone group of Met172 (5.33) and the chloro atom stabilized the compound in the binding site.

The arylolethynyl substituent at the C2 position of **34** was oriented toward the extracellular part of the  $A_3$ AR in close proximity to TM2.  $A_{2A}$ AR is characterized by four constraining disulfide bridges in the extracellular domains, unlike the  $A_3$ AR, which has only one disulfide bond in that region. Thus, we expected the  $A_3$ AR to be more subject to reorganization of the TMs. The disulfide bond between Cys77 (3.25) and Cys166 (EL2) is conserved not only among the AR subtypes but also among the family A GPCRs, and it is crucial for the expression and the function of the receptors. This disulfide bond involving Cys166 holds in place the backbone of two neighboring EL2 residues that are important in ligand coordination, i.e., Gln167 and Phe168. Two other disulfide bridges of  $A_{2A}$ AR are between EL1 and EL2, namely, between Cys71 and Cys159 and

between Cys74 and Cys146. Another disulfide bond involves the two cysteines in EL3, Cys259, and Cys262. It has been speculated that the presence within the extracellular domains of the three disulfide bridges unique to  $A_{2A}$ AR is not crucial for the tertiary structure and the stability of the receptor but is indeed important for ligand recognition.<sup>39</sup> From the structural point of view, from a comparison between the  $A_{2A}$ AR structure and other GPCR structures, the presence of the two disulfide bridges between EL1 and EL2 forced the extracellular terminal of TM2 toward the TM bundle, thus reducing the size of the pocket embedding the agonist C2-substituents.

The IFD procedure applied to these rigid, extended  $A_3$ AR agonists at the  $A_{2A}$ AR-based model of  $A_3$ AR was unable to accommodate the long and straight arylolethynyl substituent at the C2 position due to a steric clash with the TM2 residues. In particular, the phenyl ring of the  $N^6$ -methyl 2-phenylethynyl derivative **9**, a high affinity agonist at  $A_3$ AR, was clearly clashing with Ser73 in TM2, suggesting that the orientations of the extracellular terminal of TM2 and the EL1 in the  $A_{2A}$ AR-based model of  $A_3$ AR were not optimal for the accessibility of these methanocarpa derivatives to the  $A_3$ AR binding site.

New hybrid models of the  $A_3$ AR (Figure 3) were built using different templates for the homology modeling of the extracellular part of TM2, namely, an agonist-bound human  $\beta_2$  adrenergic receptor crystallographic structure (designated  $A_3$ AR- $\beta_2$ adr)<sup>40</sup> and the structure of the opsin in the activated state (designated  $A_3$ AR-ops).<sup>41</sup> In the hybrid  $A_3$ AR model based on both the  $A_{2A}$ AR and the  $\beta_2$ -adrenergic receptor structures, the extracellular extremity of TM2 moved outward by about 4 Å at the  $C\alpha$  atom of Ser73. This movement created a larger pocket for the C2 arylolethynyl substituents of the  $A_3$ AR agonists, thereby allowing derivatives such as agonist **9** to dock in the binding cavity without steric clashes with TM2. Nevertheless, the docking of the  $N^6$ -methyl 2-biphenylethynyl agonist **24** to the binding site of the  $A_3$ AR- $\beta_2$ adr model did not produce any reasonable pose due to the steric clash between the distal phenyl ring of the compound and the residues in TM2. The unfit docked pose of **24** to the  $A_3$ AR- $\beta_2$ adr model of  $A_3$ AR suggested that a larger pocket for the longer C2-substituted agonists was needed.

The outward movement of the extracellular terminal of TM2 in the hybrid A<sub>3</sub>AR-ops model was by approximately 7 Å at the Cα of Ser73, with the creation of a larger pocket for the accessibility of C2 substituents of the present rigid chain-extended A<sub>3</sub>AR agonists, such as compounds **24** and **34**. The docking poses of **24** and **34** in the A<sub>3</sub>AR-ops model showed the biphenylethynyl moiety of the C2 chain pointing toward the extracellular environment. The dihedral angle between the two phenyl rings was approximately 30–40°, making the C2 chain noncoplanar with the ethynyl moiety. The biphenylethynyl side chain was stabilized by favorable hydrophobic interactions with residues in TM2, EL2, and TM7, namely, Ile268 (7.39), Tyr265 (7.36), Val72 (2.64), Leu264 (7.35), Phe168 (EL2), and the carbon chain of Gln167 (EL2). The side chain of Gln167, after the IFD optimization, pointed away from the binding cavity, opening the cavity to the agonists. The docking pose of **34** showed the distal phenyl ring of the C2 chain between the carbon chain of Gln167 and the aromatic ring of Tyr265. Tyr265 is in the wall of the binding pocket, but  $\pi$  interactions with the ligand were not evident. Analogue **22**, which deviated from planarity because of the branched *t*-Bu group, was significantly less potent in hA<sub>3</sub>AR binding. The presence of a halogen atom at the *o*-, *m*-, or *p*-positions of the phenyl ring in the C2 chain was studied in the binding sites of A<sub>3</sub>AR models and the A<sub>2A</sub>AR crystal structure in order to understand the gain of affinity of compounds **15** and **30** at the A<sub>2A</sub>AR. The *m*-Cl atoms of the C2 side chain of **15** and **30** in the predicted orientations in the A<sub>3</sub>AR-ops model were located between Tyr271 and Gln167 (EL2), locked in the pocket by interactions between the halogen atom of the compounds and the OH group of Tyr271 and the side chain CO group of Gln167. The corresponding residue of Gln167 in human A<sub>2A</sub>AR is the hydrophobic and bulky Leu167. Nevertheless, in the docked poses of compounds **15** and **30** in the binding site of A<sub>2A</sub>AR, the *m*-Cl atom was able to generate strong interactions with the hydroxyl groups and the aromatic moieties of Tyr271 (7.35) and Tyr9 (1.35) of A<sub>2A</sub>AR. Instead, the orientation of the *o*-Cl atom of the docked agonists **14** and **29** was not optimal to create interactions with the side chain of Tyr271 (7.35) of A<sub>2A</sub>AR. However, in the docked complexes of **14** and **29** with the A<sub>3</sub>AR-ops model, the *o*-Cl atom was located between Tyr265 (7.35) and Val169 (EL2), creating favorable interactions with the OH group of Tyr265 and the backbone NH group of Val169. The residue corresponding to Val169 in the A<sub>2A</sub>AR is Glu169, whose side chain was oriented such that the  $\gamma$ -carboxyl group interacted with the backbone NH group, i.e., no longer available to interact with the *o*-Cl atom of **14** or **29**.

## DISCUSSION

In previous studies,<sup>13</sup> the SAR in AR binding was studied for two series of ribonucleosides that are particularly suited for selectivity at the hA<sub>3</sub>AR: N<sup>6</sup>-methyl and N<sup>6</sup>-3-halobenzyl. N<sup>6</sup>-3-Halobenzyl substitution is greatly favored for maintaining the selectivity of ribosides at the A<sub>3</sub>AR in mouse and rat. Upon addition of the (*N*)-methanocarba modification,<sup>21</sup> a rise in affinity was observed at the mA<sub>1</sub>AR for certain 2-chloroadenine analogues, leading to a reduction of AR selectivity in murine species. However, straight chain alkynyl groups at the C2 position, such as pentynyl **7**, alleviated this problem by reducing affinity at the mA<sub>1</sub>AR. Substitution with 2-arylethynyl groups was not examined in the (*N*)-methanocarba series of A<sub>3</sub>AR

agonists by Melman et al.,<sup>21</sup> but we have introduced this modification in the present study.

Previously, in the ribose-5'-uronamide series, combination of 2-phenylalkynyl groups with various bulky N<sup>6</sup> substituents was not additive in its effect on A<sub>3</sub>AR affinity. In a series of A<sub>3</sub>AR-selective N<sup>6</sup>-arylurea derivatives, a 2-phenylalkynyl group reduced the rA<sub>3</sub>AR affinity in comparison to a 2-chloro analogue containing the same bulky N<sup>6</sup>-arylurea, although selectivity was increased.<sup>42</sup> The combination of N<sup>6</sup>-(substituted benzyl) groups and a 2-phenylethynyl modification produced much lower affinity in hA<sub>3</sub>AR binding than the same structure with H at the C2 position.<sup>24</sup> A study of 2-pyrazolyl-N<sup>6</sup>-substituted adenosine derivatives concluded that bulky substitutions at those two positions generally did not benefit from additivity in hA<sub>3</sub>AR binding affinity.<sup>13c</sup>

We have now explored the effects of various 2-(arylethynyl) groups at the adenine C2 position on AR affinity of (*N*)-methanocarba 5'-*N*-methyluronamido nucleosides. The resulting analogues (both N<sup>6</sup>-methyl and N<sup>6</sup>-3-halobenzyl) were full agonists of the hA<sub>3</sub>AR of nanomolar affinity that were consistently highly selective (typically >1000-fold vs hA<sub>1</sub>AR and hA<sub>2A</sub>AR). The most potent and selective N<sup>6</sup>-methyl compounds were *p*-F **13** and *o*-Cl **14** analogues. At the mA<sub>3</sub>AR, selectivity generally remained, but for N<sup>6</sup>-methyl derivatives, the high affinities achievable were somewhat lower than those at hA<sub>3</sub>AR. Thus, the combination of a 2-(arylethynyl) group and large N<sup>6</sup> substitutions was better tolerated at the A<sub>3</sub>AR in the methanocarba series than in the 9-ribose series, as characterized in earlier reports. There is also a broad flexibility of substitution of the 2-(arylethynyl) moiety, with halo, hydrophobic, and hydrophilic substitutions without losing A<sub>3</sub>AR selectivity. This feature could also benefit specific pharmacological characteristics, such as pharmacokinetic properties. The 3,4-difluoro substitution of **31** might impede possible *in vivo* metabolic transformation of this ring (cf. P2Y<sub>12</sub> receptor antagonist Ticagrelor<sup>1b</sup>).

The pharmacokinetic properties of these analogues have not been measured. However, they represent an increase in hydrophobicity, as well as selectivity, in comparison to most widely used A<sub>3</sub>AR agonists. For example, the cLog P values of potent 2-chlorophenylethynyl **29**, 4-fluorophenylethynyl **30**, and 3,4-fluorophenylethynyl **31** derivatives are 4.65, 4.08, and 4.15, respectively. The cLog P values of more polar ribosides **1** and **2** are 0.48 and 1.20, respectively, which is possibly less desirable for full bioavailability. The total polar surface area of **29** is 121.9 Å<sup>2</sup>, which is a more favorable value for one of the physical parameters that predicts drug-likeness compared to 131.1 Å<sup>2</sup> for both **1** and **2**.<sup>43</sup>

Even large, planar polyaromatic groups at C2 (separated by an acetylene moiety) were tolerated and retained nanomolar affinity. In binding to the A<sub>2A</sub>AR, a 2-(2-(naphth-1-yl)-ethoxy) analogue bound with high affinity, and the location of the naphthyl group was predicted by docking.<sup>44</sup> In the present study, the size of the polycyclic C2 groups, i.e., in the potent phenanthrene-ethynyl derivative **26**, exceeded that of all previous AR ligands. The 1-pyrene derivative **35** and its less potent 4-pyrene isomer **36** represent different sites of attachment of the 2-ethynyl moiety to the same large polyaromatic group. In receptor binding experiments, differences were observed that could provide insight into the geometry of the binding site considering the spatial and conformational constraints of these agonists. The 4-pyrene



derivative **36** (with one additional ring added) has a close analogue in the  $N^6$ -methyl series, i.e., **26**.

These observations were subjected to molecular modeling analysis, which also predicted useful analogues to be synthesized. The ribose moiety is tightly anchored through a H-bond network involving TM3 and TM7, and the geometry of the unnatural glycosidic bond to the nucleobase is restricted. Thus, there is little angular flexibility of the extended, rigid C2 substituents. Thus, anchoring of the adenosine moiety to conserved amino acid residues provides a framework for exploring the region surrounding the linearly extended C2 substituent. The placement of a 2-arylethynyl substituent in the  $hA_3AR$  binding site was predicted by Dal Ben et al. using the inactive structure of the  $hA_{2A}AR$  as template, and the orientation is similar to that found here.<sup>23b</sup> However, the present study predicts the docking mode with greater detail and confidence because the homology model is based on the agonist-bound  $A_{2A}AR$  structure.<sup>23</sup> With the present set of rigidified analogues, we have located a very large hydrophobic pocket on the receptor that depends on an outward displacement of TM2 in order to accommodate multiple fused rings. Thus, the binding would be allowed by the plasticity of the receptor structure to attain a ligand-specific reorganization. The reduction of  $hA_3AR$  affinity for the larger C2 substituents in **35** and **36** suggests that although TM2 could shift position to accommodate such groups, there is an energetic cost for these more bulky planar polyaromatic groups. As the movement of TM2 increases, some stabilizing interactions with other regions of the receptor would be progressively lost.

The  $A_3AR$  homology model built based exclusively on the crystal structure of an agonist-bound  $A_{2A}AR$  required an adjustment of the position of TM2, which was based on the orientation of TM2 in other agonist-bound or activated GPCR templates, i.e., the  $\beta_2$ -adrenergic receptor or opsin. The most successful template for TM2 was the structure of opsin, which displaced the upper part of TM2 relative to the agonist-bound  $A_{2A}AR$  by  $\sim 7$  Å. Thus, we predict an outward displacement of TM2 similar to the opsin structure, which is specific for agonists containing rigid C2 extensions. The inability of the  $A_{2A}AR$  to undergo this rearrangement might contribute to the  $A_3AR$  selectivity of these compounds.

The displacement of one or more TMs to accommodate a sterically bulky ligand, assuming that there are no other constraints on the helix such as a proximal disulfide bond, might be a general phenomenon in GPCRs. The ability of the helices to readjust position or “breathe” to enable a larger ligand to bind has already been proposed, specifically with respect to the “multi-conformational space of the antagonist-like state of the human  $A_3$  receptor”.<sup>45</sup> The example of altered  $A_{2A}AR$  conformation specific to the binding of a sterically extended agonist 6-(2,2-diphenylethylamino)-9-((2*R*,3*R*,4*S*,5*S*)-5-(ethylcarbamoyl)-3,4-dihydroxytetrahydrofuran-2-yl)-*N*-(2-(3-(1-(pyridin-2-yl)piperidin-4-yl)ureido)ethyl)-9*H*-purine-2-carboxamide (**59**, UK-432097) was already documented in the X-ray structure.<sup>25</sup> In particular, outward movements of EL3 and extracellular portion of TM7 were associated exclusively with this bulky, multifunctionalized agonist.

The implications for receptor coupling and signaling of this type of displacement, such as the agonist-dependent movement of TM2 that we predict here, are unknown. If this conformational change associated with a family of ligands is propagated to the intracellular regions, we speculate that there

could be differential effects on multiple signaling pathways and might eventually provide a rational basis for the design of biased GPCR agonists.

The enhancement of  $A_{2A}AR$  affinity in the 2-(3-chlorophenylethynyl) analogues **15** and **30** indicated a consistent interaction with a specific site on the  $hA_{2A}AR$ . Modeling analysis suggested halogen- $\pi$  interactions<sup>46</sup> with two tyrosine residues in the C2 binding cavity of  $A_{2A}AR$ , namely, Tyr271 (7.36) and Tyr9 (1.35), to explain the activity of the 2-(3-chlorophenylethynyl) methanocarb adenosine derivatives **15** and **30** at the  $A_{2A}AR$ .

The freedom to insert polyaromatic ring systems on the 2-ethynyl group suggests inclusion of reporter groups, such as fluorescent dye moieties at this site. In fact, the pyren-1-yl analogue **35** is highly fluorescent and could be explored as spectroscopic probes of moderate affinity for receptor binding experiments. The fluorescent properties of pyrene are sensitive to the environment. The *p*-amino derivative **32** has a high affinity at both the  $mA_3AR$  and  $hA_3AR$ , and could potentially be derivatized for radioisotope incorporation or affinity cross-linking. We are also interested in the design of radiofluorinated nucleosides for positron emission tomographic (PET) imaging of the  $A_3AR$  in vivo.<sup>47</sup> Several fluorinated species in this study could provide the basis for incorporation of  $^{18}F$  into a high affinity  $A_3AR$  agonist.

In conclusion, we have found a new series of highly potent and selective series of  $A_3AR$  agonists containing combined substitution of the (*N*)-methanocarb ring system and arylethynyl groups at the adenine C2 position. The binding affinities demonstrated high tolerance of steric bulk and ring substitution by extension at the C2 position, with many aryl groups providing  $K_i$  values in the nanomolar range. Molecular modeling suggests that this reflects conformational plasticity of the  $A_3AR$ . Potent agonist ligands should be useful in future pharmacological studies of the antiinflammatory, anticancer, and antiischemic properties of  $A_3AR$  agonists.

## ■ EXPERIMENTAL SECTION

**Chemical Synthesis. Materials and Instrumentation.** *L*-Ribose and other reagents and solvents were purchased from Sigma-Aldrich (St. Louis, MO). Alcohol derivative **39** was prepared as reported.<sup>28</sup>  $^1H$  NMR spectra were obtained with a Bruker 400 spectrometer using  $CDCl_3$  and  $CD_3OD$  as solvents. Chemical shifts are expressed in  $\delta$  values (ppm) with tetramethylsilane ( $\delta$  0.00) for  $CDCl_3$  and water ( $\delta$  3.30) for  $CD_3OD$ . TLC analysis was carried out on glass sheets precoated with silica gel  $F_{254}$  (0.2 mm) from Aldrich. The purity of final nucleoside derivatives was checked using a Hewlett-Packard 1100 HPLC equipped with a Zorbax SB-Aq 5  $\mu m$  analytical column (50  $\times$  4.6 mm; Agilent Technologies Inc., Palo Alto, CA). Mobile phase: linear gradient solvent system, 5 mM TBAP (tetrabutylammonium dihydrogenphosphate)- $CH_3CN$  from 80:20 to 0:100 in 13 min; the flow rate was 0.5 mL/min. Peaks were detected by UV absorption with a diode array detector at 230, 254, and 280 nm. All derivatives tested for biological activity showed >95% purity by HPLC analysis (detection at 254 nm). Low-resolution mass spectrometry was performed with a JEOL SX102 spectrometer with 6-kV Xe atoms following desorption from a glycerol matrix or on an Agilent LC/MS 1100 MSD, with a Waters (Milford, MA) Atlantis C18 column. High resolution mass spectroscopic (HRMS) measurements were performed on a proteomics optimized Q-TOF-2 (Micromass-Waters) using external calibration with polyalanine, unless noted. Observed mass accuracies are those expected based on known performance of the instrument as well as trends in masses of standard compounds observed at intervals during the series of measurements. Reported masses are observed masses uncorrected for this time-dependent drift

in mass accuracy. Synthetic procedures for 45–47 are in Supporting Information. LogP and total polar surface area values were calculated using ChemBioDraw Ultra (version 12.0.3, PerkinElmer, Boston, MA).

(1*S*,2*R*,3*S*,4*R*,5*S*)-2,3-Dihydroxy-*N*-methyl-4-(6-(methylamino)-2-(phenylethynyl)-9*H*-purin-9-yl)bicyclo[3.1.0]hexane-1-carboxamide (9). A solution of compound 45a (29 mg, 0.06 mmol) in methanol (2 mL) and 10% trifluoromethane sulfonic acid (2 mL) was heated at 70 °C for 5 h. The solvent was evaporated under vacuum, and the residue was purified on flash silica gel column chromatography (CH<sub>2</sub>Cl<sub>2</sub>/MeOH = 25:1) to give compound 9 (21 mg, 81%) as a syrup. <sup>1</sup>H NMR (CD<sub>3</sub>OD) δ 8.12 (s, 1H), 7.67–7.65 (m, 2H), 7.47–7.43 (m, 2H), 5.06 (d, *J* = 5.2 Hz, 1H), 4.08 (d, *J* = 6.4 Hz, 1H), 3.15 (br s, 3H), 2.84 (s, 3H), 2.13–2.10 (m, 1H), 1.88 (t, *J* = 5.2 Hz, 1H), 1.41–1.39 (m, 1H). HRMS calculated for C<sub>22</sub>H<sub>23</sub>N<sub>6</sub>O<sub>3</sub> (M + H)<sup>+</sup>: 419.1832; found, 419.1818.

(1*S*,2*R*,3*S*,4*R*,5*S*)-2,3-Dihydroxy-*N*-methyl-4-(6-(methylamino)-2-(pyridin-2-ylethynyl)-9*H*-purin-9-yl)bicyclo[3.1.0]hexane-1-carboxamide (10). Compound 10 (80%) was prepared from compound 46 following the same method as that used for compound 9. <sup>1</sup>H NMR (CD<sub>3</sub>OD) δ 8.65 (s, 1H), 8.01 (s, 1H), 7.91–7.97 (m, 1H), 7.87 (d, *J* = 8.8 Hz, 1H), 7.53–7.48 (m, 1H), 5.15 (d, *J* = 5.6 Hz, 1H), 4.09 (d, *J* = 8.4 Hz, 1H), 3.14 (br s, 3H), 2.83 (s, 3H), 2.13–2.06 (m, 1H), 1.85 (t, *J* = 5.2 Hz, 1H), 1.42–1.40 (m, 1H). HRMS calculated for C<sub>21</sub>H<sub>22</sub>N<sub>7</sub>O<sub>3</sub> (M + H)<sup>+</sup>: 420.1784; found, 420.1797.

(1*S*,2*R*,3*S*,4*R*,5*S*)-4-(2-((2-Fluorophenyl)ethynyl)-6-(methylamino)-9*H*-purin-9-yl)-2,3-dihydroxy-*N*-methylbicyclo[3.1.0]hexane-1-carboxamide (11). Compound 11 (82%) was prepared from compound 45b following the same method as that used for compound 9. <sup>1</sup>H NMR (CD<sub>3</sub>OD) δ 8.11 (s, 1H), 7.49–7.39 (m, 3H), 7.25–7.20 (m, 1H), 5.06 (d, *J* = 5.2 Hz, 1H), 4.9 (s, 1H), 4.02 (d, *J* = 6.8 Hz, 1H), 3.15 (br s, 1H), 2.84 (s, 3H), 2.13–2.10 (m, 1H), 1.88 (t, *J* = 4.8 Hz, 1H), 1.41–1.38 (m, 1H). HRMS calculated for C<sub>22</sub>H<sub>22</sub>FN<sub>6</sub>O<sub>3</sub> (M + H)<sup>+</sup>: 437.1737; found, 437.1753.

(1*S*,2*R*,3*S*,4*R*,5*S*)-4-(2-((3-Fluorophenyl)ethynyl)-6-(methylamino)-9*H*-purin-9-yl)-2,3-dihydroxy-*N*-methylbicyclo[3.1.0]hexane-1-carboxamide (12). Compound 12 (78%) was prepared from compound 45c following the same method as that used for compound 9. <sup>1</sup>H NMR (CD<sub>3</sub>OD) δ 8.11 (s, 1H), 7.67 (t, *J* = 6.0 Hz, 1H), 7.52–7.47 (m, 1H), 7.28–7.22 (m, 2H), 5.07 (d, *J* = 6.8 Hz, 1H), 4.03 (d, *J* = 6.8 Hz, 1H), 3.13 (br s, 1H), 2.84 (s, 3H), 2.13–2.10 (m, 1H), 1.88 (t, *J* = 4.8 Hz, 1H), 1.41–1.40 (m, 1H). HRMS calculated for C<sub>22</sub>H<sub>22</sub>FN<sub>6</sub>O<sub>3</sub> (M + H)<sup>+</sup>: 437.1737; found, 437.1718.

(1*S*,2*R*,3*S*,4*R*,5*S*)-4-(2-((4-Fluorophenyl)ethynyl)-6-(methylamino)-9*H*-purin-9-yl)-2,3-dihydroxy-*N*-methylbicyclo[3.1.0]hexane-1-carboxamide (13). Compound 13 (81%) was prepared from compound 45d following the same method as that used for compound 9. <sup>1</sup>H NMR (CD<sub>3</sub>OD) δ 8.11 (s, 1H), 7.75–7.68 (m, 2H), 7.23–7.18 (m, 2H), 5.05 (d, *J* = 6.0 Hz, 1H), 4.02 (d, *J* = 6.4 Hz, 1H), 3.14 (br s, 3H), 2.84 (s, 3H), 2.13–2.10 (m, 1H), 1.89 (t, *J* = 4.8 Hz, 1H), 1.41–1.39 (m, 1H). HRMS calculated for C<sub>22</sub>H<sub>22</sub>FN<sub>6</sub>O<sub>3</sub> (M + H)<sup>+</sup>: 437.1737; found, 437.1722.

(1*S*,2*R*,3*S*,4*R*,5*S*)-4-(2-((2-Chlorophenyl)ethynyl)-6-(methylamino)-9*H*-purin-9-yl)-2,3-dihydroxy-*N*-methylbicyclo[3.1.0]hexane-1-carboxamide (14). Compound 14 (85%) was prepared from compound 45e following the same method as that used for compound 9. <sup>1</sup>H NMR (CD<sub>3</sub>OD) δ 8.11 (s, 1H), 7.72 (d, *J* = 7.2 Hz, 1H), 7.54 (d, *J* = 7.2 Hz, 1H), 7.46–7.36 (m, 2H), 5.10 (d, *J* = 6.4 Hz, 1H), 4.04 (d, *J* = 6.8 Hz, 1H), 3.15 (br s, 3H), 2.83 (s, 3H), 2.12–2.08 (m, 1H), 1.86 (t, *J* = 4.8 Hz, 1H), 1.41–1.39 (m, 1H). HRMS calculated for C<sub>22</sub>H<sub>22</sub>ClN<sub>6</sub>O<sub>3</sub> (M + H)<sup>+</sup>: 453.1442; found, 453.1449.

(1*S*,2*R*,3*S*,4*R*,5*S*)-4-(2-((3-Chlorophenyl)ethynyl)-6-(methylamino)-9*H*-purin-9-yl)-2,3-dihydroxy-*N*-methylbicyclo[3.1.0]hexane-1-carboxamide (15). Compound 15 (82%) was prepared from compound 45f following the same method as that used for compound 9. <sup>1</sup>H NMR (CD<sub>3</sub>OD) δ 8.11 (s, 1H), 7.67 (s, 1H), 7.59 (d, *J* = 7.2 Hz, 1H), 7.49–7.42 (m, 2H), 5.06 (d, *J* = 6.4 Hz, 1H), 4.02 (d, *J* = 6.8 Hz, 1H), 3.14 (br s, 3H), 2.84 (s, 3H), 2.13–2.10 (m, 1H), 1.88 (t, *J* = 4.8 Hz, 1H), 1.41–1.39 (m, 1H). HRMS calculated for C<sub>22</sub>H<sub>22</sub>ClN<sub>6</sub>O<sub>3</sub> (M + H)<sup>+</sup>: 453.1442; found, 453.1442.

(1*S*,2*R*,3*S*,4*R*,5*S*)-4-(2-((4-Chlorophenyl)ethynyl)-6-(methylamino)-9*H*-purin-9-yl)-2,3-dihydroxy-*N*-methylbicyclo[3.1.0]hexane-1-carboxamide (16). Compound 16 (84%) was prepared from compound 45g following the same method as that used for compound 9. <sup>1</sup>H NMR (CD<sub>3</sub>OD) δ 8.10 (s, 1H), 7.64 (d, *J* = 8.4 Hz, 2H), 7.46 (d, *J* = 8.4 Hz, 2H), 5.06 (d, *J* = 5.6 Hz, 1H), 4.88 (s, 1H), 4.02 (d, *J* = 6.4 Hz, 1H), 3.15 (br s, 3H), 2.84 (s, 3H), 2.13–2.09 (m, 1H), 1.88 (t, *J* = 4.8 Hz, 1H), 1.41–1.38 (m, 1H). HRMS calculated for C<sub>22</sub>H<sub>22</sub>ClN<sub>6</sub>O<sub>3</sub> (M + H)<sup>+</sup>: 453.1460; found, 453.1454.

(1*S*,2*R*,3*S*,4*R*,5*S*)-4-(2-((4-Bromophenyl)ethynyl)-6-(methylamino)-9*H*-purin-9-yl)-2,3-dihydroxy-*N*-methylbicyclo[3.1.0]hexane-1-carboxamide (17). Compound 17 (76%) was prepared from compound 45h following the same method as that used for compound 9. <sup>1</sup>H NMR (CD<sub>3</sub>OD) δ 8.10 (s, 1H), 7.62 (d, *J* = 8.8 Hz, 2H), 7.56 (d, *J* = 8.4 Hz, 2H), 5.05 (d, *J* = 6.8 Hz, 1H), 4.88 (s, 1H), 4.02 (d, *J* = 6.4 Hz, 1H), 3.14 (br s, 3H), 2.84 (s, 3H), 2.13–2.09 (m, 1H), 1.88 (t, *J* = 5.2 Hz, 1H), 1.41–1.38 (m, 1H). HRMS calculated for C<sub>22</sub>H<sub>22</sub>BrN<sub>6</sub>O<sub>3</sub> (M + H)<sup>+</sup>: 497.0937; found, 497.0948.

(1*S*,2*R*,3*S*,4*R*,5*S*)-4-(2-((3-Aminophenyl)ethynyl)-6-(methylamino)-9*H*-purin-9-yl)-2,3-dihydroxy-*N*-methylbicyclo[3.1.0]hexane-1-carboxamide (18). Compound 18 (67%) was prepared from compound 45i following the same method as that used for compound 9. <sup>1</sup>H NMR (CD<sub>3</sub>OD) δ 8.09 (s, 1H), 7.14 (t, *J* = 8.0 Hz, 1H), 6.98–6.94 (m, 2H), 6.80–6.78 (m, 1H), 5.06 (d, *J* = 5.6 Hz, 1H), 4.02 (d, *J* = 6.4 Hz, 1H), 3.15 (br s, 3H), 2.85 (s, 3H), 2.12–2.09 (m, 1H), 1.87 (t, *J* = 4.8 Hz, 1H), 1.41–1.39 (m, 1H). HRMS calculated for C<sub>22</sub>H<sub>22</sub>N<sub>7</sub>O<sub>3</sub> (M + H)<sup>+</sup>: 432.1784; found, 432.1799.

(1*S*,2*R*,3*S*,4*R*,5*S*)-4-(2-((3,4-Difluorophenyl)ethynyl)-6-(methylamino)-9*H*-purin-9-yl)-2,3-dihydroxy-*N*-methylbicyclo[3.1.0]hexane-1-carboxamide (19). Compound 19 (83%) was prepared from compound 45j following the same method as that used for compound 9. <sup>1</sup>H NMR (CD<sub>3</sub>OD) δ 8.12 (s, 1H), 7.58–7.50 (m, 1H), 7.50–7.48 (m, 1H), 7.40–7.34 (m, 1H), 5.06 (d, *J* = 6.4 Hz, 1H), 4.02 (d, *J* = 6.4 Hz, 1H), 3.14 (br s, 3H), 2.84 (s, 3H), 2.13–2.09 (m, 1H), 1.88 (t, *J* = 4.8 Hz, 1H), 1.41–1.40 (m, 1H). HRMS calculated for C<sub>22</sub>H<sub>21</sub>F<sub>2</sub>N<sub>6</sub>O<sub>3</sub> (M + H)<sup>+</sup>: 455.1643; found, 455.1639.

(1*S*,2*R*,3*S*,4*R*,5*S*)-4-(2-((3,5-Difluorophenyl)ethynyl)-6-(methylamino)-9*H*-purin-9-yl)-2,3-dihydroxy-*N*-methylbicyclo[3.1.0]hexane-1-carboxamide (20). Compound 20 (84%) was prepared from compound 45k following the same method as that used for compound 9. <sup>1</sup>H NMR (CD<sub>3</sub>OD) δ 8.12 (s, 1H), 7.31–7.26 (s, 2H), 7.14–7.09 (m, 1H), 7.49–7.42 (m, 2H), 5.06 (d, *J* = 5.2 Hz, 1H), 4.89 (s, 1H), 4.03 (d, *J* = 6.4 Hz, 1H), 3.14 (br s, 3H), 2.84 (s, 3H), 2.12–2.09 (m, 1H), 1.88 (t, *J* = 4.8 Hz, 1H), 1.41–1.39 (m, 1H). HRMS calculated for C<sub>22</sub>H<sub>21</sub>F<sub>2</sub>N<sub>6</sub>O<sub>3</sub> (M + H)<sup>+</sup>: 455.1643; found, 455.1630.

(1*S*,2*R*,3*S*,4*R*,5*S*)-4-(2-((4-Ethylphenyl)ethynyl)-6-(methylamino)-9*H*-purin-9-yl)-2,3-dihydroxy-*N*-methylbicyclo[3.1.0]hexane-1-carboxamide (21). Compound 21 (79%) was prepared from compound 45l following the same method as that used for compound 9. <sup>1</sup>H NMR (CD<sub>3</sub>OD) δ 8.09 (s, 1H), 7.57 (d, *J* = 8.0 Hz, 2H), 7.29 (d, *J* = 8.0 Hz, 2H), 5.06 (d, *J* = 5.2 Hz, 1H), 4.91 (s, 1H), 4.02 (d, *J* = 6.4 Hz, 1H), 3.15 (br s, 3H), 2.84 (s, 3H), 2.74–2.68 (m, 2H), 2.13–2.09 (m, 1H), 1.88 (t, *J* = 4.8 Hz, 1H), 1.41–1.38 (m, 1H), 1.30 (t, *J* = 7.6 Hz, 3H). HRMS calculated for C<sub>24</sub>H<sub>27</sub>N<sub>6</sub>O<sub>3</sub> (M + H)<sup>+</sup>: 447.2145; found, 447.2130.

(1*S*,2*R*,3*S*,4*R*,5*S*)-4-(2-((4-*tert*-Butylphenyl)ethynyl)-6-(methylamino)-9*H*-purin-9-yl)-2,3-dihydroxy-*N*-methylbicyclo[3.1.0]hexane-1-carboxamide (22). Compound 22 (83%) was prepared from compound 45m following the same method as that used for compound 9. <sup>1</sup>H NMR (CD<sub>3</sub>OD) δ 8.10 (s, 1H), 7.59 (d, *J* = 8.4 Hz, 2H), 7.50 (d, *J* = 8.4 Hz, 2H), 5.06 (d, *J* = 6.4 Hz, 1H), 4.02 (d, *J* = 6.4 Hz, 1H), 3.15 (br s, 3H), 2.85 (s, 3H), 2.13–2.10 (m, 1H), 1.88 (t, *J* = 4.8 Hz, 1H), 1.41–1.39 (m, 10H). HRMS calculated for C<sub>26</sub>H<sub>31</sub>N<sub>6</sub>O<sub>3</sub> (M + H)<sup>+</sup>: 475.2458; found, 475.2450.

(1*S*,2*R*,3*S*,4*R*,5*S*)-4-(2-((4-Acetylphenyl)ethynyl)-6-(methylamino)-9*H*-purin-9-yl)-2,3-dihydroxy-*N*-methylbicyclo[3.1.0]hexane-1-carboxamide (23). Compound 23 (80%) was prepared from compound 45n following the same method as that used for compound 9. <sup>1</sup>H NMR (CD<sub>3</sub>OD) δ 8.11 (s, 1H), 8.06 (d, *J* = 8.4 Hz, 2H), 7.77 (d, *J* = 8.0 Hz, 2H), 5.06 (d, *J* = 6.4 Hz, 1H), 4.03 (d, *J* = 6.4 Hz, 1H), 3.15 (br s, 3H), 2.84 (s, 3H), 2.64 (s, 3H), 2.14–2.10 (m, 1H), 1.88 (t, *J* =



4.8 Hz, 1H), 1.41–1.39 (m, 1H). HRMS calculated for  $C_{24}H_{25}N_6O_4$  (M + H)<sup>+</sup>: 461.1937; found, 461.1937.

(1*S*,2*R*,3*S*,4*R*,5*S*)-4-(2-(Biphenyl-4-ylethynyl)-6-(methylamino)-9*H*-purin-9-yl)-2,3-dihydroxy-*N*-methylbicyclo[3.1.0]hexane-1-carboxamide (**24**). Compound **24** (74%) was prepared from compound **45o** following the same method as that used for compound **9**. <sup>1</sup>H NMR (CD<sub>3</sub>OD) δ 8.11 (s, 1H), 7.75–7.67 (m, 6H), 7.47 (t, *J* = 7.6 Hz, 2H), 7.38 (t, *J* = 7.2 Hz, 1H), 5.06 (d, *J* = 6.0 Hz, 1H), 4.89 (s, 1H), 4.03 (d, *J* = 6.4 Hz, 1H), 3.16 (br s, 3H), 2.84 (s, 3H), 2.13–2.10 (m, 1H), 1.89 (t, *J* = 4.8 Hz, 1H), 1.42–1.39 (m, 1H). HRMS calculated for  $C_{28}H_{27}N_6O_3$  (M + H)<sup>+</sup>: 495.2145; found, 495.2141.

(1*S*,2*R*,3*S*,4*R*,5*S*)-2,3-Dihydroxy-*N*-methyl-4-(6-(methylamino)-2-(naphthalen-1-ylethynyl)-9*H*-purin-9-yl)bicyclo[3.1.0]hexane-1-carboxamide (**25**). Compound **25** (73%) was prepared from compound **45p** following the same method as that used for compound **9**. <sup>1</sup>H NMR (CD<sub>3</sub>OD) δ 8.56 (d, *J* = 7.6 Hz, 1H), 8.11 (s, 1H), 8.00–7.90 (m, 3H), 7.68 (t, *J* = 5.6 Hz, 1H), 7.62–7.53 (m, 2H), 5.10 (d, *J* = 5.2 Hz, 1H), 4.93 (s, 1H), 4.06 (d, *J* = 6.4 Hz, 1H), 3.19 (br s, 3H), 2.79 (s, 3H), 2.15–2.12 (m, 1H), 1.89 (t, *J* = 4.8 Hz, 1H), 1.41–1.38 (m, 1H). HRMS calculated for  $C_{26}H_{25}N_6O_3$  (M + H)<sup>+</sup>: 469.1988; found, 469.2005.

(1*S*,2*R*,3*S*,4*R*,5*S*)-2,3-Dihydroxy-*N*-methyl-4-(6-(methylamino)-2-(phenanthren-9-ylethynyl)-9*H*-purin-9-yl)bicyclo[3.1.0]hexane-1-carboxamide (**26**). Compound **26** (65%) was prepared from compound **45q** following the same method as that used for compound **9**. <sup>1</sup>H NMR (CD<sub>3</sub>OD) δ 8.84–8.77 (m, 2H), 8.66–8.63 (m, 1H), 8.26 (s, 1H), 8.12 (s, 1H), 7.97 (d, *J* = 7.6 Hz, 1H), 7.80–7.73 (m, 3H), 7.66 (t, *J* = 7.2 Hz, 1H), 5.10 (d, *J* = 6.0 Hz, 1H), 4.92 (s, 1H), 4.07 (d, *J* = 6.4 Hz, 1H), 3.20 (br s, 3H), 2.81 (s, 3H), 2.15–2.12 (m, 1H), 1.90 (t, *J* = 4.8 Hz, 1H), 1.42–1.38 (m, 1H). HRMS calculated for  $C_{30}H_{27}N_6O_3$  (M + H)<sup>+</sup>: 519.2145; found, 519.2137.

(1*S*,2*R*,3*S*,4*R*,5*S*)-4-(6-(3-Chlorobenzylamino)-2-(phenylethynyl)-9*H*-purin-9-yl)-2,3-dihydroxy-*N*-methylbicyclo[3.1.0]hexane-1-carboxamide (**27**). PdCl<sub>2</sub>(PPh<sub>3</sub>)<sub>2</sub> (6.13 mg, 0.008 mmol), CuI (1.2 mg, 0.004 mmol), phenylacetylene (30 μL, 0.26 mmol), and triethylamine (60 μL, 0.4 mmol) were added to a solution of compound **44** (26 mg, 0.04 mmol) in anhydrous DMF (1 mL) and stirred at room temperature overnight. The solvent was evaporated under vacuum, and the residue was roughly purified on flash silica gel column chromatography. The resulting compound was dissolved in methanol (2 mL) and 10% trifluoromethane sulfonic acid (2 mL), and heated at 70 °C for 5 h. The solvent was evaporated under vacuum, and the residue was purified on flash silica gel column chromatography (CH<sub>2</sub>Cl<sub>2</sub>/MeOH = 25:1) to give compound **27** (17 mg, 76%) as a syrup. <sup>1</sup>H NMR (CD<sub>3</sub>OD) δ 8.13 (s, 1H), 7.66–7.63 (m, 2H), 7.46–7.42 (m, 4H), 7.37–7.26 (m, 3H), 5.06 (d, *J* = 5.6 Hz, 1H), 4.9 (br s, 2H), 4.04 (d, *J* = 6.4 Hz, 1H), 2.84 (s, 3H), 2.14–2.11 (m, 1H), 1.88 (t, *J* = 4.8 Hz, 1H), 1.41–1.37 (m, 1H). HRMS calculated for  $C_{28}H_{26}ClN_6O_3$  (M + H)<sup>+</sup>: 529.1755; found, 529.1740.

(1*S*,2*R*,3*S*,4*R*,5*S*)-4-(6-(3-Chlorobenzylamino)-2-(4-fluorophenyl)ethynyl)-9*H*-purin-9-yl)-2,3-dihydroxy-*N*-methylbicyclo[3.1.0]hexane-1-carboxamide (**28**). Compound **28** (68%) was prepared from compound **44** following the same method as that used for compound **27**. <sup>1</sup>H NMR (CD<sub>3</sub>OD) δ 8.13 (s, 1H), 7.70–7.63 (m, 2H), 7.59–7.55 (m, 1H), 7.45 (s, 1H), 7.37–7.21 (m, 3H), 7.19–7.16 (m, 1H), 5.06 (d, *J* = 5.6 Hz, 1H), 4.9 (s, 1H), 4.58 (br s, 2H), 4.04 (d, *J* = 7.6 Hz, 1H), 2.84 (s, 3H), 2.17–2.10 (m, 1H), 1.88 (t, *J* = 4.8 Hz, 1H), 1.41–1.38 (m, 1H). HRMS calculated for  $C_{28}H_{25}ClFN_6O_3$  (M + H)<sup>+</sup>: 547.1661; found, 547.1652.

(1*S*,2*R*,3*S*,4*R*,5*S*)-4-(6-(3-Chlorobenzylamino)-2-((2-chlorophenyl)ethynyl)-9*H*-purin-9-yl)-2,3-dihydroxy-*N*-methylbicyclo[3.1.0]hexane-1-carboxamide (**29**). Compound **29** (65%) was prepared from compound **44** following the same method as that used for compound **27**. <sup>1</sup>H NMR (CD<sub>3</sub>OD) δ 8.14 (s, 1H), 7.72–7.70 (m, 1H), 7.53 (d, *J* = 8.0 Hz, 1H), 7.47–7.25 (m, 6H), 5.11 (d, *J* = 6.8 Hz, 1H), 4.90 (s, 1H), 4.05 (d, *J* = 6.8 Hz, 1H), 2.82 (s, 3H), 2.12–2.09 (m, 1H), 1.86 (t, *J* = 4.8 Hz, 1H), 1.40–1.38 (m, 1H). HRMS calculated for  $C_{28}H_{24}Cl_2N_6O_3Na$  (M + Na)<sup>+</sup>: 585.1185; found, 585.1167.

(1*S*,2*R*,3*S*,4*R*,5*S*)-4-(6-(3-Chlorobenzylamino)-2-((3-chlorophenyl)ethynyl)-9*H*-purin-9-yl)-2,3-dihydroxy-*N*-

methylbicyclo[3.1.0]hexane-1-carboxamide (**30**). Compound **30** (66%) was prepared from compound **44** following the same method as that used for compound **27**. <sup>1</sup>H NMR (CD<sub>3</sub>OD) δ 8.15 (s, 1H), 7.66–7.57 (m, 2H), 7.48–7.26 (m, 6H), 5.07 (d, *J* = 6.4 Hz, 1H), 4.85 (s, 1H), 4.04 (d, *J* = 6.8 Hz, 1H), 2.84 (s, 3H), 2.14–2.10 (m, 1H), 1.88 (t, *J* = 4.8 Hz, 1H), 1.41–1.39 (m, 1H). HRMS calculated for  $C_{28}H_{25}Cl_2N_6O_3$  (M + H)<sup>+</sup>: 563.1365; found, 563.1359.

(1*S*,2*R*,3*S*,4*R*,5*S*)-4-(6-(3-Chlorobenzylamino)-2-((3,4-difluorophenyl)ethynyl)-9*H*-purin-9-yl)-2,3-dihydroxy-*N*-methylbicyclo[3.1.0]hexane-1-carboxamide (**31**). Compound **31** (63%) was prepared from compound **44** following the same method as that used for compound **27**. <sup>1</sup>H NMR (CD<sub>3</sub>OD) δ 8.14 (s, 1H), 7.58 (t, *J* = 8.8 Hz, 1H), 7.47–7.44 (m, 2H), 7.39–7.25 (m, 4H), 5.06 (d, *J* = 6.4 Hz, 1H), 4.89 (s, 1H), 4.04 (d, *J* = 6.4 Hz, 1H), 2.84 (s, 3H), 2.13–2.10 (m, 1H), 1.88 (t, *J* = 4.8 Hz, 1H), 1.41–1.38 (m, 1H). HRMS calculated for  $C_{28}H_{24}F_2ClN_6O_3$  (M + H)<sup>+</sup>: 565.1566; found, 565.1559.

(1*S*,2*R*,3*S*,4*R*,5*S*)-4-(2-((4-Aminophenyl)ethynyl)-6-(3-chlorobenzylamino)-9*H*-purin-9-yl)-2,3-dihydroxy-*N*-methylbicyclo[3.1.0]hexane-1-carboxamide (**32**). Compound **32** (59%) was prepared from compound **44** following the same method as that used for compound **27**. <sup>1</sup>H NMR (CD<sub>3</sub>OD) δ 8.02 (s, 1H), 7.84 (d, *J* = 8.8 Hz, 2H), 7.33–7.23 (m, 4H), 6.60 (d, *J* = 8.4 Hz, 2H), 5.17 (d, *J* = 6.4 Hz, 1H), 4.85 (s, 1H), 4.73 (br s, 2H), 4.02 (d, *J* = 6.8 Hz, 1H), 2.83 (s, 3H), 2.08–2.05 (m, 1H), 1.81 (t, *J* = 4.8 Hz, 1H), 1.41–1.37 (m, 1H). HRMS calculated for  $C_{28}H_{27}ClN_7O_3$  (M + H)<sup>+</sup>: 545.1041; found, 545.1045.

3-((6-(3-Chlorobenzylamino)-9-((1*S*,2*R*,3*S*,4*R*,5*S*)-3,4-dihydroxy-5-(methyl-carbamoyl)bicyclo[3.1.0]hexane-2-yl)-9*H*-purin-2-yl)ethynyl)benzoic acid (**33**). PdCl<sub>2</sub>(PPh<sub>3</sub>)<sub>2</sub> (3.0 mg, 0.004 mmol), CuI (1.0 mg, 0.004 mmol), phenylacetylene (18.7 mg, 0.12 mmol), and triethylamine (20 μL, 0.2 mmol) were added to a solution of compound **44** (12.68 mg, 0.02 mmol) in anhydrous DMF (1 mL) and stirred at room temperature overnight. The solvent was evaporated under vacuum, and the residue was roughly purified on flash silica gel column chromatography. The resulting compound was dissolved in dioxane (2 mL) and 1 N HCl (1.5 mL), and heated at 60 °C for 2 h. After completion of the starting material, the solvent was evaporated under vacuum, and the residue was purified on flash silica gel column chromatography (CH<sub>2</sub>Cl<sub>2</sub>/MeOH/TFA = 25:1:0.1) to give compound **33** (7 mg, 61%) as a syrup. <sup>1</sup>H NMR (CD<sub>3</sub>OD) δ 8.28 (s, 1H), 8.18–8.16 (m, 1H), 8.11–8.07 (m, 1H), 7.87 (d, *J* = 7.6 Hz, 1H), 7.59–7.54 (m, 2H), 7.47 (s, 1H), 7.41–7.26 (m, 2H), 5.09 (d, *J* = 6.4 Hz, 1H), 4.91 (s, 1H), 4.05 (d, *J* = 6.4 Hz, 1H), 2.85 (s, 3H), 2.14–2.11 (m, 1H), 1.88 (t, *J* = 4.8 Hz, 1H), 1.42–1.38 (m, 1H). HRMS calculated for  $C_{29}H_{26}ClN_6O_5$  (M + H)<sup>+</sup>: 573.1653; found, 573.1646.

(1*S*,2*R*,3*S*,4*R*,5*S*)-4-(2-(Biphenyl-4-ylethynyl)-6-(3-chlorobenzylamino)-9*H*-purin-9-yl)-2,3-dihydroxy-*N*-methylbicyclo[3.1.0]hexane-1-carboxamide (**34**). Compound **34** (68%) was prepared from compound **44** following the same method as that used for compound **27**. <sup>1</sup>H NMR (CD<sub>3</sub>OD) δ 8.13 (s, 1H), 7.74–7.66 (m, 7H), 7.49–7.45 (m, 2H), 7.40–7.26 (m, 4H), 5.07 (d, *J* = 5.6 Hz, 1H), 4.9 (s, 1H), 4.60 (br s, 2H), 4.05 (d, *J* = 6.4 Hz, 1H), 2.85 (s, 3H), 2.14–2.11 (m, 1H), 1.89 (t, *J* = 4.8 Hz, 1H), 1.42–1.40 (m, 1H). HRMS calculated for  $C_{34}H_{30}ClN_6O_3$  (M + H)<sup>+</sup>: 605.2068; found, 605.2083.

(1*S*,2*R*,3*S*,4*R*,5*S*)-4-(6-(3-Chlorobenzylamino)-2-(pyren-1-ylethynyl)-9*H*-purin-9-yl)-2,3-dihydroxy-*N*-methylbicyclo[3.1.0]hexane-1-carboxamide (**35**). Compound **35** (91%) was prepared from compound **44** following the same method as that used for compound **33**. <sup>1</sup>H NMR (CD<sub>3</sub>OD) δ 8.71 (d, *J* = 9.2 Hz, 1H), 8.26–8.23 (m, 4H), 8.16–8.13 (m, 2H), 8.08–8.03 (m, 3H), 7.54 (s, 1H), 7.43 (d, *J* = 7.6 Hz, 1H), 7.34 (t, *J* = 8.0 Hz, 1H), 7.27 (d, *J* = 8.0 Hz, 1H), 5.06 (d, *J* = 6.4 Hz, 1H), 4.83 (s, 1H), 4.04 (d, *J* = 6.4 Hz, 1H), 2.81 (s, 3H), 2.10–2.07 (m, 1H), 1.89 (t, *J* = 4.8 Hz, 1H), 1.41–1.37 (m, 1H). HRMS calculated for  $C_{38}H_{30}ClN_6O_3$  (M + H)<sup>+</sup>: 653.2068; found, 653.2078.

(1*S*,2*R*,3*S*,4*R*,5*S*)-4-(6-(3-Chlorobenzylamino)-2-(pyren-4-ylethynyl)-9*H*-purin-9-yl)-2,3-dihydroxy-*N*-methylbicyclo[3.1.0]hexane-1-carboxamide (**36**). Compound **36** (69%) was prepared from compound **44** following the same method as that used for compound **33**. <sup>1</sup>H NMR (CD<sub>3</sub>OD) δ 8.82 (d, *J* = 7.6 Hz, 1H), 8.51 (s, 1H),

8.29–8.21 (m, 3H), 8.16–8.12 (m, 4H), 8.04 (t,  $J = 7.6$  Hz, 1H), 7.54 (s, 1H), 7.43 (d,  $J = 7.6$  Hz, 1H), 7.35 (t,  $J = 8.0$  Hz, 1H), 7.28 (d,  $J = 8.4$  Hz, 1H), 5.1 (d,  $J = 6.0$  Hz, 1H), 4.06 (d,  $J = 6.0$  Hz, 1H), 2.80 (s, 3H), 2.18–2.09 (m, 1H), 1.89 (t,  $J = 4.8$  Hz, 1H), 1.42–1.39 (m, 1H). HRMS calculated for  $C_{38}H_{30}ClN_6O_3$  ( $M + H$ )<sup>+</sup>: 653.2068; found, 653.2056.

(1*S*,2*R*,3*S*,4*R*,5*S*)-Ethyl-(2,3-*O*-isopropylidene)-4-(2-iodo-6-(methylamino)-9*H*-purin-9-yl)bicyclo[3.1.0]hexane-1-carboxylate (**41**). Methylamine hydrochloride (0.353 g, 5.23 mmol) and triethylamine (1.4 mL, 16.6 mmol) was added to a solution of compound **40** (0.528 g, 1.04 mmol) in anhydrous methanol (15 mL) and stirred at room temperature overnight. The solvent was evaporated under vacuum, and the residue was purified on flash silica gel column chromatography (hexane/ethylacetate = 1:1) to give compound **41** (0.470 g, 94%) as a foamy solid. <sup>1</sup>H NMR ( $CD_3OD$ )  $\delta$  7.94 (s, 1H), 5.83 (d,  $J = 7.2$  Hz, 1H), 4.94 (s, 1H), 4.80 (d,  $J = 6.0$  Hz, 1H), 4.33–4.27 (m, 2H), 3.05 (br s, 3H), 2.25–2.21 (m, 1H), 1.65–1.61 (m, 1H), 1.53–1.49 (m, 4H), 1.34 (t,  $J = 7.2$  Hz, 3H), 1.29 (s, 3H). HRMS calculated for  $C_{18}H_{23}IN_5O_4$  ( $M + H$ )<sup>+</sup>: 500.1072; found, 500.1075.

(1*S*,2*R*,3*S*,4*R*,5*S*)-(2,3-*O*-isopropylidene)-4-(2-iodo-6-(methylamino)-9*H*-purin-9-yl)-*N*-methylbicyclo[3.1.0]hexane-1-carboxamide (**43**). 40% Methylamine solution (10 mL) was added to a solution of compound **41** (0.470 g, 0.94 mmol) in methanol (15 mL) and stirred at room temperature for 48 h. The solvent was evaporated under vacuum, and the residue was purified on flash silica gel column chromatography ( $CH_2Cl_2/MeOH = 40:1$ ) to give compound **43** (0.360 g, 79%) as a syrup. <sup>1</sup>H NMR ( $CD_3OD$ )  $\delta$  7.95 (s, 1H), 5.72 (d,  $J = 7.2$  Hz, 1H), 4.93 (s, 1H), 4.84 (d,  $J = 7.2$  Hz, 1H), 3.05 (br s, 3H), 2.90 (s, 3H), 2.17–2.11 (m, 1H), 1.54–1.49 (m, 4H), 1.39 (t,  $J = 5.2$  Hz, 1H), 1.30 (s, 3H). HRMS calculated for  $C_{17}H_{22}IN_6O_3$  ( $M + H$ )<sup>+</sup>: 485.0798; found, 485.0803.

**Pharmacological Characterization.** The nucleoside derivatives, dissolved as stock solutions in DMSO (5 mM) and stored frozen, were evaluated in binding<sup>29–31</sup> and a functional assay<sup>34</sup> at the  $A_3AR$ , binding assays at the  $A_1AR$  and  $A_{2A}AR$ , and a functional assay at the  $hA_3AR$  (details in Supporting Information). Use of heterologously expressed mouse ARs was as reported.<sup>33b,49</sup> Protein content was determined<sup>48</sup> and  $IC_{50}$  values in binding inhibition transformed to  $K_i$  values<sup>50</sup> as reported.

**Molecular Modeling.** The Homology Model module of MOE was utilized to build a new molecular model of the  $hA_3AR$  (details in Supporting Information). The recently reported model of the complex of the nonselective AR agonist **59** docked to the crystal structure of the  $A_{2A}AR$  was used as a template for modeling of the  $A_3AR$ .<sup>25,51</sup> The sequence alignment of the  $A_{2A}$  and  $A_3AR$ s was performed with MOE, taking into account positions of highly conserved amino acid residues. The position of full agonist **59** inside the  $A_{2A}AR$  was taken into account during the modeling. In the resulting initial homology model of the  $A_3AR$  (prior to movement of TM2), the complex 5',2', $N^6$  trisubstituted agonist **59** used to crystallize the  $A_{2A}AR$  was removed and the simpler 5'-uronamide **58** docked inside the receptor. The Glide program of the Schrodinger package<sup>52</sup> was used to dock the other agonists to the  $A_3AR$  model obtained. The receptor grid generation was performed for the box with a center in the centroid of **58** in its initial position. The size of the box was determined automatically. The extra precision mode (XP) of Glide was used for the docking. The binding site was defined as **58** and all amino acid residues located within 5 Å from **58**. All  $A_3AR$  residues located within 2 Å from the binding site were used as a shell. The following parameters of energy minimization were used: OPLS2005 force field, water was used as an implicit solvent, and a maximum of 5000 iterations of the Polak–Ribier conjugate gradient minimization method was used with a convergence threshold of  $0.01 \text{ kJ}\cdot\text{mol}^{-1}\cdot\text{\AA}^{-1}$ . Another reference nucleoside **58** was also docked in this  $hA_3AR$  homology model.

Hybrid  $A_3AR$  models involving movement of TM2, as explained above, were utilized to study the binding mode of analogue **34** and all other novel analogues in Table 1 using induced fit docking implemented in the Schrödinger package. Grid generation was performed for a cubic box with sides of 26 Å and having a center in

the centroid of the agonist molecules. The default values were used for other parameters.

## ■ ASSOCIATED CONTENT

### Supporting Information

Docking figures for compounds **14**, **15**, and **34**, procedures for the synthesis of intermediates, detailed molecular modeling procedures, and biological assays for novel nucleoside derivatives, and coordinates of complexes with **13**, **31**, and **35**. This material is available free of charge via the Internet at <http://pubs.acs.org>.

## ■ AUTHOR INFORMATION

### Corresponding Author

\*Molecular Recognition Section, Bldg. 8A, Rm. B1A-19, NIH, NIDDK, LBC, Bethesda, MD 20892-0810. Tel: 301-496-9024. Fax: 301-480-8422. E-mail: [kajacobs@helix.nih.gov](mailto:kajacobs@helix.nih.gov).

### Author Contributions

<sup>§</sup>These authors contributed equally to this work.

### Notes

The authors declare no competing financial interest.

## ■ ACKNOWLEDGMENTS

We thank Dr. John Lloyd and Dr. Noel Whittaker (NIDDK) for mass spectral determinations. This research was supported by the Intramural Research Program of the NIH, National Institute of Diabetes and Digestive and Kidney Diseases, and by NIH R01 HL077707.

## ■ ABBREVIATIONS

AR, adenosine receptor; cAMP, adenosine 3',5'-cyclic phosphate; CHO, Chinese hamster ovary; Cl-IB-MECA, 2-chloro- $N^6$ -(3-iodobenzyl)-5'-*N*-methylcarboxamidoadenosine; DIPEA, diisopropylethylamine; DCM, dichloromethane; DMF, *N,N*-dimethylformamide; DMEF, Dulbecco's modified Eagle's medium; EDTA, ethylenediaminetetraacetic acid; EL, extracellular loop; GPCR, G protein-coupled receptor; HEK, human embryonic kidney; I-AB-MECA,  $N^6$ -(4-amino-3-iodobenzyl)-adenosine-5'-*N*-methyl-uronamide; IFD, induced fit docking; NECA, 5'-*N*-ethylcarboxamidoadenosine; HEPES, 4-(2-hydroxyethyl)-1-piperazineethanesulfonic acid; HRMS, high resolution mass spectroscopy; NMR, nuclear magnetic resonance; R-PIA,  $N^6$ -*R*-phenylisopropyladenosine; TEA, triethylamine; TLC, thin layer chromatography; TM, transmembrane domain

## ■ REFERENCES

- (1) (a) Cheong, S. L.; Federico, S.; Venkatesan, G.; Mandel, A. L.; Shao, Y. M.; Moro, S.; Spalluto, G.; Pastorin, G. The  $A_3$  adenosine receptor as multifaceted therapeutic target: pharmacology, medicinal chemistry, and in silico approaches. *Med. Res. Rev.* **2012**, DOI: 10.1002/med.20254. (b) Jacobson, K. A.; Balasubramanian, R.; Deflorian, F.; Gao, Z. G. G protein-coupled adenosine (P1) and P2Y receptors. *Purinergic Signalling* **2012**, DOI: 10.1007/s11302-012-9294-7.
- (2) Fishman, P.; Jacobson, K. A.; Ochaion, A.; Cohen, S.; Bar-Yehuda, S. The anti-cancer effect of  $A_3$  adenosine receptor agonists: A novel, targeted therapy. *Immunol. Endocr. Metab. Agents Med. Chem.* **2007**, *7*, 298–303.
- (3) Silverman, M. H.; Strand, V.; Markovits, D.; Nahir, M.; Reitblat, T.; Molad, Y.; Rosner, I.; Rozenbaum, M.; Mader, R.; Adawi, M.; Caspi, D.; Tishler, M.; Langevitz, P.; Rubinow, A.; Friedman, J.; Green, L.; Tanay, A.; Ochaion, A.; Cohen, S.; Kerns, W. D.; Cohn, I.; Fishman-Furman, S.; Farbstein, M.; Bar-Yehuda, S.; Fishman, P. Clinical evidence for utilization of the  $A_3$  adenosine receptor as a target



to treat rheumatoid arthritis: Data from a phase II clinical trial. *J. Rheumatol.* **2008**, *35*, 41–48.

(4) Gessi, S.; Merighi, S.; Varani, K.; Cattabriga, E.; Benini, A.; Mirandola, P.; Leung, E.; MacLennan, S.; Feo, C.; Baraldi, S.; Borea, P. A. Adenosine receptors in colon carcinoma tissues and colon tumoral cell lines: focus on the A<sub>3</sub> adenosine subtype. *J. Cell. Physiol.* **2007**, *211*, 826–836.

(5) Zheng, J.; Wang, R.; Zambraski, E.; Wu, D.; Jacobson, K. A.; Liang, B. T. A novel protective action of adenosine A<sub>3</sub> receptors: Attenuation of skeletal muscle ischemia and reperfusion injury. *Am. J. Physiol.: Heart Circ. Physiol.* **2007**, *293*, 3685–3691.

(6) Wan, T. C.; Ge, Z. D.; Tampo, A.; Mio, Y.; Bienengraeber, M. W.; Tracey, W. R.; Gross, G. J.; Kwok, W. M.; Auchampach, J. A. The A<sub>3</sub> adenosine receptor agonist CP-532,903 [*N*<sup>6</sup>-(2,5-dichlorobenzyl)-3'-aminoadenosine-5'-*N*-methylcarboxamide] protects against myocardial ischemia/reperfusion injury via the sarcolemmal ATP-sensitive potassium channel. *J. Pharmacol. Exp. Ther.* **2008**, *324*, 234–243.

(7) Guzman, J.; Yu, J. G.; Suntres, Z.; Bozarov, A.; Cooke, H.; Javed, N.; Auer, H.; Palatini, J.; Hassanain, H. H.; Cardounel, A. J.; Javed, A.; Grants, I.; Wunderlich, J. E.; Christofi, F. L. ADOA3R as a therapeutic target in experimental colitis: Proof by validated high-density oligonucleotide microarray analysis. *Inflamm. Bowel Dis.* **2006**, *12*, 766–789.

(8) (a) Fishman, P.; Bar-Yehuda, S.; Liang, B. T.; Jacobson, K. A. Pharmacological and therapeutic effects of A<sub>3</sub> adenosine receptor (A<sub>3</sub>AR) agonists. *Drug Discovery Today* **2012**, *17*, 359–366. (b) Gessi, S.; Merighi, S.; Varani, K.; Leung, E.; MacLennan, S.; Borea, P. A. The A<sub>3</sub> adenosine receptor: An enigmatic player in cell biology. *Pharmacol. Ther.* **2008**, *117*, 123–140.

(9) Yamano, K.; Inoue, M.; Masaki, S.; Saki, M.; Ichimura, M.; Satoh, M. Generation of adenosine A<sub>3</sub> receptor functionally humanized mice for the evaluation of the human antagonists. *Biochem. Pharmacol.* **2006**, *71*, 294–306.

(10) Yang, H.; Avila, M. Y.; Peterson-Yantorno, K.; Coca-Prados, M.; Stone, R. A.; Jacobson, K. A.; Civan, M. M. The cross-species A<sub>3</sub> adenosine-receptor antagonist MRS 1292 inhibits adenosine-triggered human nonpigmented ciliary epithelial cell fluid release and reduces mouse intraocular pressure. *Curr. Eye Res.* **2005**, *30*, 747–754.

(11) Hua, X.; Chason, K. D.; Fredholm, B. B.; Deshpande, D. A.; Penn, R. B.; Tilley, S. L. Adenosine induces airway hyperresponsiveness through activation of A<sub>3</sub> receptors on mast cells. *J. Allergy Clin. Immunol.* **2008**, *122*, 107–113.

(12) Bulger, E. M.; Tower, C. M.; Warner, K. J.; Garland, T.; Cuschieri, J.; Rizoli, S.; Rhind, S.; Junger, W. G. Increased neutrophil adenosine A<sub>3</sub> receptor expression is associated with hemorrhagic shock and injury severity in trauma patients. *Shock* **2011**, *36*, 435–439.

(13) (a) Gao, Z. G.; Kim, S. K.; Biadatti, T.; Chen, W.; Lee, K.; Barak, D.; Kim, S. G.; Johnson, C. R.; Jacobson, K. A. Structural determinants of A<sub>3</sub> adenosine receptor activation: Nucleoside ligands at the agonist/antagonist boundary. *J. Med. Chem.* **2002**, *45*, 4471–4484. (b) Jeong, L. S.; Lee, H. W.; Jacobson, K. A.; Kim, H. O.; Shin, D. H.; Lee, J. A.; Gao, Z. G.; Lu, C.; Duong, H. T.; Gunaga, P.; Lee, S. K.; Jin, D. Z.; Chun, M. W.; Moon, H. R. Structure-activity relationships of 2-chloro-*N*<sup>6</sup>-substituted-4'-thioadenosine-5'-uronamides as highly potent and selective agonists at the human A<sub>3</sub> adenosine receptor. *J. Med. Chem.* **2006**, *49*, 273–281. (c) Elzein, E.; Palle, V.; Wu, Y.; Maa, T.; Zeng, D.; Zablocki, J. 2-Pyrazolyl-*N*<sup>6</sup>-substituted adenosine derivatives as high affinity and selective adenosine A<sub>3</sub> receptor agonists. *J. Med. Chem.* **2004**, *47*, 4766–4773. (d) DeNinno, M. P.; Masamune, H.; Chenard, L. K.; DiRico, K. J.; Eller, C.; Etienne, J. B.; Tickner, J. E.; Kennedy, S. P.; Knight, D. R.; Kong, J.; Oleynek, J. J.; Tracey, W. R.; Hill, R. J. The synthesis of highly potent, selective, and water-soluble agonists at the human adenosine A<sub>3</sub> receptor. *Bioorg. Med. Chem. Lett.* **2006**, *16*, 2525–2527. (e) Cosyn, L.; Palaniappan, K. K.; Kim, S. K.; Duong, H. T.; Gao, Z. G.; Jacobson, K. A.; Van Calenbergh, S. 2-Triazole-substituted adenosines: A new class of selective A<sub>3</sub> adenosine receptor agonists, partial agonists, and antagonists. *J. Med. Chem.* **2006**, *49*, 7373–7383.

(14) Jacobson, K. A.; Ji, X.-d.; Li, A. H.; Melman, N.; Siddiqui, M. A.; Shin, K. J.; Marquez, V. E.; Ravi, R. G. Methanocarba analogues of purine nucleosides as potent and selective adenosine receptor agonists. *J. Med. Chem.* **2000**, *43*, 2196–2203.

(15) Lee, K.; Ravi, R. G.; Ji, X.-d.; Marquez, V. E.; Jacobson, K. A. Ring-constrained (*N*)methanocarba-nucleosides as adenosine receptor agonists: Independent 5'-uronamide and 2'-deoxy modifications. *Bioorg. Med. Chem. Lett.* **2001**, *11*, 1333–1337.

(16) Tchilibon, S.; Joshi, B. V.; Kim, S. K.; Duong, H. T.; Gao, Z. G.; Jacobson, K. A. Methanocarba 2,*N*<sup>6</sup>-disubstituted adenine nucleosides as highly potent and selective A<sub>3</sub> adenosine receptor agonists. *J. Med. Chem.* **2005**, *48*, 1745–1758.

(17) Ochaion, A.; Bar-Yehuda, S.; Cohen, S.; Amital, H.; Jacobson, K. A.; Joshi, B. V.; Gao, Z. G.; Barer, F.; Patoka, R.; Del Valle, L.; Perez-Liz, G.; Fishman, P. The A<sub>3</sub> adenosine receptor agonist CF502 inhibits the PI3K, PKB/Akt and NF-κkB signaling pathway in synoviocytes from rheumatoid arthritis patients and in adjuvant induced arthritis rats. *Biochem. Pharmacol.* **2008**, *76*, 482–494.

(18) Matot, I.; Weininger, C. F.; Zeira, E.; Galun, E.; Joshi, B. V.; Jacobson, K. A. A<sub>3</sub> Adenosine receptors and mitogen activated protein kinases in lung injury following in-vivo reperfusion. *Critical Care* **2006**, *10*, R65.

(19) Chen, Z.; Janes, K.; Chen, C.; Doyle, T.; Tosh, D. K.; Jacobson, K. A.; Salvemini, D. Controlling murine and rat chronic pain through A<sub>3</sub> adenosine receptor activation. *FASEB J.* **2012**, DOI: 10.1096/fj.11-201541.

(20) (a) Volpini, R.; Dal Ben, D.; Lambertucci, C.; Taffi, S.; Vittori, S.; Klotz, K. N.; Cristalli, G. J. *N*<sup>6</sup>-Methoxy-2-alkynyladenosine derivatives as highly potent and selective ligands at the human A<sub>3</sub> adenosine receptor. *J. Med. Chem.* **2007**, *50*, 1222–1230. (b) Cristalli, G.; Lambertucci, C.; Marucci, G.; Volpini, R.; Dal Ben, D. A<sub>3A</sub> Adenosine receptor and its modulators: Overview on a druggable GPCR and on structure-activity relationship analysis and binding requirements of agonists and antagonists. *Curr. Pharm. Des.* **2008**, *14*, 1525–1552.

(21) Melman, A.; Gao, Z. G.; Kumar, D.; Wan, T. C.; Gizewski, E.; Auchampach, J. A.; Jacobson, K. A. Design of (*N*)-methanocarba adenosine 5'-uronamides as species-independent A<sub>3</sub> receptor-selective agonists. *Bioorg. Med. Chem. Lett.* **2008**, *18*, 2813–2819.

(22) Dooley, M. J.; Quinn, R. J. The three binding domain model of adenosine receptors: molecular modeling aspects. *J. Med. Chem.* **1992**, *35*, 211–217.

(23) (a) Volpini, R.; Buccioni, M.; Dal Ben, D.; Lambertucci, C.; Lammi, C.; Marucci, G.; Ramadori, A. T.; Klotz, K. N.; Cristalli, G. Synthesis and biological evaluation of 2-alkynyl-*N*<sup>6</sup>-methyl-5'-*N*-methylcarboxamidoadenosine derivatives as potent and highly selective agonists for the human adenosine A<sub>3</sub> receptor. *J. Med. Chem.* **2009**, *52*, 7897–7900. (b) Dal Ben, D.; Lambertucci, C.; Lammi, C.; Marucci, G.; Thomas, A.; Volpini, R.; Cristalli, G. Molecular modeling study on potent and selective adenosine A<sub>3</sub> receptor agonists. *Bioorg. Med. Chem.* **2010**, *18*, 7923–7930.

(24) Seviliano, L. G.; McGuigan, C.; Davies, R. H. Compounds useful as A<sub>3</sub> adenosine receptor agonists. U.S. Patent 7,414,036 B2, 2008.

(25) Xu, F.; Wu, H.; Katritch, V.; Han, G. W.; Jacobson, K. A.; Gao, Z. G.; Cherezov, V.; Stevens, R. C. Structure of an agonist-bound human A<sub>2A</sub> adenosine receptor. *Science* **2011**, *332*, 322–327.

(26) Congreve, M.; Langmead, C. J.; Mason, J. S.; Marshall, F. H. Progress in structure based drug design for G protein-coupled receptors. *J. Med. Chem.* **2011**, *54*, 4283–4311.

(27) Chinchilla, R.; Nájera, C. The Sonogashira reaction: A booming methodology in synthetic organic chemistry. *Chem. Rev.* **2007**, *107*, 874–922.

(28) Tosh, D. K.; Chinn, M.; Ivanov, A. A.; Klutz, A. M.; Gao, Z. G.; Jacobson, K. A. Functionalized congeners of A<sub>3</sub> adenosine receptor-selective nucleosides containing a bicyclo[3.1.0]hexane ring system. *J. Med. Chem.* **2009**, *52*, 7580–7592.

(29) Schwabe, U.; Trost, T. Characterization of adenosine receptors in rat brain by (-)-[<sup>3</sup>H]*N*<sup>6</sup>-phenylisopropyladenosine. *Naunyn-Schmiedeberg Arch. Pharmacol.* **1989**, *313*, 179–187.

- (30) Jarvis, M. F.; Schutz, R.; Hutchison, A. J.; Do, E.; Sills, M. A.; Williams, M. [<sup>3</sup>H]CGS 21680, an A<sub>2</sub> selective adenosine receptor agonist directly labels A<sub>2</sub> receptors in rat brain tissue. *J. Pharmacol. Exp. Ther.* **1989**, *251*, 888–893.
- (31) Olah, M. E.; Gallo-Rodriguez, C.; Jacobson, K. A.; Stiles, G. L. [<sup>125</sup>I]-4-Aminobenzyl-5'-N-methylcarboxamidoadenosine, a high affinity radioligand for the rat A<sub>3</sub> adenosine receptor. *Mol. Pharmacol.* **1994**, *45*, 978–982.
- (32) Englert, M.; Quitterer, U.; Klotz, K. N. Effector coupling of stably transfected human A<sub>3</sub> adenosine receptors in CHO cells. *Biochem. Pharmacol.* **2002**, *64*, 61–65.
- (33) (a) Jacobson, K. A.; Park, K. S.; Jiang, J.-I.; Kim, Y. C.; Olah, M. E.; Stiles, G. L.; Ji, X. d. Pharmacological characterization of novel A<sub>3</sub> adenosine receptor-selective antagonists. *Neuropharmacology* **1997**, *36*, 1157–1165. (b) Ge, Z. D.; Peart, J. N.; Kreckler, L. M.; Wan, T. C.; Jacobson, M. A.; Gross, G. J.; Auchampach, J. A. Cl-IB-MECA [2-chloro-N<sup>6</sup>-(3-iodobenzyl)adenosine-5'-N-methylcarboxamide] reduces ischemia/reperfusion injury in mice by activating the A<sub>3</sub> adenosine receptor. *J. Pharmacol. Exp. Ther.* **2006**, *319*, 1200–1210.
- (34) Nordstedt, C.; Fredholm, B. B. A modification of a protein-binding method for rapid quantification of cAMP in cell-culture supernatants and body fluid. *Anal. Biochem.* **1990**, *189*, 231–234.
- (35) Sherman, W.; Day, T.; Jacobson, M. P.; Friesner, R. A.; Farid, R. Novel procedure for modeling ligand/receptor induced fit effects. *J. Med. Chem.* **2006**, *49*, 534–553.
- (36) Ivanov, A. A.; Barak, D.; Jacobson, K. A. Evaluation of homology modeling of GPCRs in light of the A<sub>2A</sub> adenosine receptor crystallographic structure. *J. Med. Chem.* **2009**, *52*, 3284–3292.
- (37) Jaakola, V. P.; Lane, J. R.; Lin, J. Y.; Katritch, V.; IJzerman, A. P.; Stevens, R. C. Ligand binding and subtype selectivity of the human A<sub>2A</sub> adenosine receptor: identification and characterization of essential amino acid residues. *J. Biol. Chem.* **2010**, *285*, 13032–13044.
- (38) Costanzi, S.; Ivanov, A. A.; Tikhonova, I. G.; Jacobson, K. A. Structure and function of G protein-coupled receptors studied using sequence analysis, molecular modeling and receptor engineering: adenosine receptors. *Front. Drug. Des. Discovery* **2007**, *3*, 63–79.
- (39) O'Malley, M. A.; Naranjo, A. N.; Lazarova, T.; Robinson, A. S. Analysis of adenosine A<sub>2A</sub> receptor stability: Effects of ligands and disulfide bonds. *Biochemistry* **2010**, *49*, 9181–9189.
- (40) Rasmussen, S. G. F.; DeVree, B. T.; Zou, Y.; Kruse, A. C.; Chung, K. Y.; Kobilka, T. S.; Thian, F. S.; Chae, P. S.; Pardon, E.; Calinski, D.; Mathiesen, J. M.; Shah, S. T. A.; Lyons, J. A.; Caffrey, M.; Gellman, S. H.; Steyaert, J.; Skiniotis, G.; Weis, W. I.; Sunihara, R. K.; Kobilka, B. K. Crystal structure of the β<sub>2</sub> adrenergic receptor–Gs protein complex. *Nature* **2011**, *477*, 549–555.
- (41) Scheerer, P.; Park, J. H.; Hildebrand, P. W.; Kim, Y. J.; Krauss, N.; Choe, H. W.; Hofmann, K. P.; Ernst, O. P. Crystal structure of opsin in its G-protein-interacting conformation. *Nature* **2008**, *455*, 497–502.
- (42) Baraldi, P. G.; Cacciari, B.; Pineda de las Infantas, M. J.; Romagnoli, R.; Spalluto, G.; Volpini, R.; Costanzi, S.; Vittori, S.; Cristalli, G.; Melman, N.; Park, K.-S.; Ji, X.-d.; Jacobson, K. A. Synthesis and biological activity of a new series of N<sup>6</sup>-arylcarbamoyl-, 2-(ar)alkynyl-N<sup>6</sup>-arylcarbamoyl, and N<sup>6</sup>-carboxamido- derivatives of adenosine-5'-N-ethyluronamide (NECA) as A<sub>1</sub> and A<sub>3</sub> adenosine receptor agonists. *J. Med. Chem.* **1998**, *41*, 3174–3185.
- (43) Bickerton, G. R.; Paolini, G. V.; Besnard, J.; Muresan, S.; Hopkins, A. L. Quantifying the chemical beauty of drugs. *Nature Chem.* **2012**, *4*, 90–98.
- (44) Deflorian, F.; Kumar, T. S.; Phan, K.; Gao, Z. G.; Xu, F.; Wu, H.; Katritch, V.; Stevens, R. C.; Jacobson, K. A. Evaluation of molecular modeling of agonist binding in light of the crystallographic structure of the agonist-bound A<sub>2A</sub> adenosine receptor. *J. Med. Chem.* **2012**, *55*, 538–552.
- (45) Moro, S.; Deflorian, F.; Bacilieri, M.; Spalluto, G. Ligand-based homology modeling as attractive tool to inspect GPCR structural plasticity. *Curr. Pharm. Des.* **2006**, *12*, 2175–2185.
- (46) Hardegger, L. A.; Kuhn, B.; Spinnler, B.; Anselm, L.; Ecabert, R.; Stihle, M.; Gsell, B.; Thoma, R.; Diez, J.; Benz, J.; Plancher, J. M.; Hartmann, G.; Banner, D. W.; Haap, W.; Diederich, F. Systematic investigation of halogen bonding in protein-ligand interactions. *Angew. Chem. Int. Ed.* **2011**, *50*, 314–318.
- (47) Kiesewetter, D. O.; Lang, L.; Ma, Y.; Bhattacharjee, A. K.; Gao, Z. G.; Joshi, B. V.; Melman, A.; Castro, S.; Jacobson, K. A. Synthesis and characterization of [<sup>76</sup>Br]-labeled high affinity A<sub>3</sub> adenosine receptor ligands for positron emission tomography. *Nucl. Med. Biol.* **2009**, *36*, 3–10.
- (48) Bradford, M. M. A rapid and sensitive method for the quantitation of microgram quantities of protein utilizing the principle of protein-dye binding. *Anal. Biochem.* **1976**, *72*, 248–254.
- (49) Kreckler, L. M.; Wan, T. C.; Ge, Z. D.; Auchampach, J. A. Adenosine inhibits tumor necrosis factor-α release from mouse peritoneal macrophages via A<sub>2A</sub> and A<sub>2B</sub> but not the A<sub>3</sub> adenosine receptors. *J. Pharmacol. Exp. Ther.* **2006**, *317*, 172–180.
- (50) Cheng, Y.-C.; Prusoff, W. H. Relationship between inhibition constant (K<sub>I</sub>) and concentration of inhibitor which causes 50% inhibition (I<sub>50</sub>) of an enzymatic-reaction. *Biochem. Pharmacol.* **1973**, *22*, 3099–3108.
- (51) Tosh, D. K.; Phan, K.; Deflorian, F.; Wei, Q.; Gao, Z. G.; Jacobson, K. A. Truncated (N)-methanocarba nucleosides as A<sub>1</sub> adenosine receptor agonists and partial agonists: overcoming lack of a recognition element. *ACS Med. Chem. Lett.* **2011**, *2*, 626–631.
- (52) Mohamadi, F. N.; Richards, G. J.; Guida, W. C.; Liskamp, R.; Lipton, M.; Caufield, C.; Chang, G.; Hendrickson, T.; Still, W. C. Macromodel an integrated software system for modeling organic and bioorganic molecules using molecular mechanics. *J. Comput. Chem.* **1990**, *11*, 440–467.